



TaTHI2 interacts with Ca²⁺-dependent protein kinase TaCPK5 to suppress virus infection by regulating ROS accumulation

Jin Yang^{1,2,†}, Lu Chen^{1,3,†}, Juan Zhang¹, Peng Liu¹, Ming Chen³ , Zhihui Chen⁴, Kaili Zhong¹, Jiaqian Liu¹, Jianping Chen^{1,*} and Jian Yang^{1,*} 

¹State Key Laboratory for Quality and Safety of Agro-products, Institute of Plant Virology, Ningbo University, Ningbo, China

²College of Plant Protection, Northwest Agriculture and Forestry University, Yangling, China

³Institute of Crop Sciences, State Key Laboratory of Crop Gene Resources and Breeding, National Key Facility for Crop Gene Resources and Genetic Improvement, Chinese Academy of Agricultural Sciences, Beijing, China

⁴School of Life Sciences, University of Dundee, Dundee, UK

Received 21 April 2023;

revised 9 November 2023;

accepted 3 December 2023.

*Correspondence (Tel +86 571 86419012;

fax +86 571 885521; email nather2008@163.com (J.Y.);

Tel +86 571 86404003; fax

+86 571 86404003; email jichen2001@126.com (J.C.))

†These authors have contributed equally to this work.

Summary

Thiamine (vitamin B1) biosynthesis involves key enzymes known as thiazole moieties (THI1/THI2), which have been shown to participate in plant responses to abiotic stress. However, the role of THI1/THI2 in plant immunity remains unclear. In this study, we cloned TaTHI2 from wheat and investigated its function in Chinese wheat mosaic virus (CWMV) infection. Overexpression of TaTHI2 (TaTHI2-OE) inhibited CWMV infection, while TaTHI2 silencing enhanced viral infection in wheat. Interestingly, the membrane-localized TaTHI2 protein was increased during CWMV infection. TaTHI2 also interacted with the Ca²⁺-dependent protein kinase 5 (TaCPK5), which is localized in the plasma membrane, and promoted reactive oxygen species (ROS) production by repressing TaCPK5-mediated activity of the catalase protein TaCAT1. CWMV CP disrupted the interaction between TaTHI2 and TaCAT1, reducing ROS accumulation and facilitating viral infection. Additionally, transgenic plants overexpressing TaTHI2 showed increased seed number per ear and 1000-kernel weight compared to control plants. Our findings reveal a novel function of TaTHI2 in plant immunity and suggest its potential as a valuable gene for balancing disease resistance and wheat yield. Furthermore, the disruption of the TaTHI2-mediated plant immune pathway by CWMV CP provides further evidence for the evolutionary arms race between plants and viruses.

Keywords: wheat, TaTHI2, TaCPK5, reactive oxygen species, Chinese wheat mosaic virus, CP.

Introduction

Plants face a range of pathogen threats during their lifecycle, including fungi, bacteria and viruses. To counter these threats, plants have evolved a strong two-tiered immune system known as pattern-triggered immunity (PTI) and effector-triggered immunity (ETI) in the co-evolutionary arms race with microbial plant pathogens (Jones and Dangl, 2006). Upon activation of PTI or ETI, plants mount downstream responses to the pathogen, such as RNA interference, cell wall reinforcement, extensive transcriptional reprogramming and reactive oxygen species (ROS) production (Bacete *et al.*, 2017; Baulcombe, 2004; Caplan *et al.*, 2008; Chang *et al.*, 2021).

ROS play a crucial role in plant immunity, serving not only as a defense molecule against viral invasion but also as a signal to activate the immune response of plants (Li *et al.*, 2021; Mittler, 2016; Mittler *et al.*, 2022). For example, the wheat yellow mosaic virus NIb protein interacts with TaVTC2 and inhibits TaVTC2 activity to produce vitamin C, leading to a burst of ROS and thereby a reduced viral infection (Zhang *et al.*, 2023b). The citrus tristeza virus (CTV) p33 protein affects virus infectivity by activating the ROS-mediated host immune response (Sun and Folimonova, 2019). However, to successfully infest plants, some viruses have evolved the ability to regulate ROS accumulation. On

the one hand, some viruses can influence the mechanism of ROS synthesis by interrupting ROS-producing enzymes (Yang *et al.*, 2017). On the other hand, some viruses can regulate the accumulation level of ROS by disrupting the activity of ROS-scavenging enzymes (Mathioudakis *et al.*, 2013).

Thiamine (vitamin B1) is a critical component of energy metabolism in all living organisms (Strobbe *et al.*, 2022). It is comprised of two parts: 4-amino-5-hydroxymethyl-2-methylpyrimidine phosphate (pyrimidine) and 4-methyl-5-(2-hydroxyethyl)-thiazole phosphate (thiazole) (Goyer, 2010). Thiazole moieties of thiamine (THI1/THI2) are essential enzymes in thiamine biosynthesis. Additionally, THI1/THI2 is a multifunctional protein that repairs DNA damage when localized in mitochondria and is involved in thiamin synthesis when localized in chloroplasts (Ajjawi *et al.*, 2007). In Arabidopsis, THI1 has been shown to modulate ABA-induced stomatal closure by interacting with Ca²⁺-dependent protein kinase at the plasma membrane (Li *et al.*, 2016). Furthermore, THI1 expression is up-regulated by abiotic stresses, such as osmotic, salinity and oxidative stress (Abidin *et al.*, 2016; Rapalakozik *et al.*, 2012; Tunc-Ozdemir *et al.*, 2009). However, it is unclear whether THI1/THI2 plays a role in plant immunity.

Chinese wheat mosaic virus (CWMV) is a member of the genus *Furovirus* in the family *Virgaviridae* (Andika *et al.*, 2013b; Diao

et al., 1999). CWMV was first reported in wheat in Shandong Province, China, in 1999 and can cause severe disease symptoms (Diao et al., 1999). CWMV has also been detected in the northern areas of Japan (Fuji et al., 2022; Maejima et al., 2010). The optimal temperature for CWMV infection was 15 ± 2 °C (Andika et al., 2013a; Yang et al., 2022). Full-length cDNA clones of CWMV have been constructed and are infectious in both wheat and *N. benthamiana* plants (Yang et al., 2016). CWMV is an RNA virus with two positive-stranded RNAs (e.g. RNA1, RNA2) and transmitted by *Polymyxa graminis* (Diao et al., 1999). CWMV RNA1 encodes three proteins: the replication-associated protein (P153, 153 kDa), RNA-dependent RNA polymerase (RdRp, 212 kDa) produced by occasional read-through of the UGA termination codon of P153, and a movement protein (MP, 37 kDa). CWMV RNA2 encodes four proteins: the major capsid protein (CP, 19 kDa), two minor CP-related proteins (N-CP, 23 kDa and CP-RT, 84 kDa) produced through initiation of translation at the noncanonical CUG start codon or through occasional read through of the UGA termination codon, respectively, and a cysteine-rich RNA-silencing suppressor protein (CRP, 19 kDa) (Andika et al., 2013a, 2013b; Diao et al., 1999; Sun et al., 2013). Previous studies have shown that a virus-derived small interfering RNA (vsiRNA-20) regulates a wheat vacuolar (*H'*)-PPases (*TaVP*) expression to promoting CWMV infection in wheat (Yang et al., 2020a). CWMV CRP phosphorylation promotes viral infection by reducing TaUBA2C RNA- and DNA-binding activity to suppress cell death and H₂O₂ production (Li et al., 2022). However, the evolutionary arms race between plants and CWMV also remains largely unknown.

In this study, we discovered that CWMV can direct TaTHI2 to the wheat cell membrane. Silencing *TaTHI2* in wheat increased susceptibility to CWMV, whereas *TaTHI2* overexpression conferred resistance against CWMV. We then investigated the role of TaTHI2 in plant immunity and found that it interacts with TaCPK5 to repress its kinase activity. Additionally, we identified TaCAT1 as a TaCPK5 substrate, with Ser-258 as an essential site for TaCAT1 activation by TaCPK5. Remarkably, TaTHI2 can increase ROS production by suppressing TaCPK5-activated TaCAT1. Furthermore, we found that CWMV CP binds competitively to TaTHI2, thereby resuming the autophosphorylation of TaCPK5 in a dose-dependent manner. In summary, TaTHI2 plays an important role in plant immunity by regulating ROS production, and CWMV CP disrupts TaTHI2-mediated host defense to facilitate CWMV infection. This study has uncovered a new pathway for regulating ROS content via TaTHI2.

Results

Characteristic analysis of TaTHI2

The full-length cDNA of the thiamine thiazole synthase gene was cloned from the cultivar Yangmai 158 of wheat (*Triticum aestivum*). The sequencing results showed that it is 1053 bp in length, and the Blast search revealed that it is identical to TraesCS7A02G376800.1. Three homologous sequences of the thiamine thiazole synthase gene exist in wheat, namely TraesCS7A02G376800.1, TraesCS7B02G278200.1 and TraesCS7D02G373100.2, and their amino acid sequences share 99.81% identity (Figure S1). To investigate the evolutionary relationship between wheat thiamine thiazole synthases and those of other species, a phylogenetic tree was constructed, and the conserved domains were analysed. The analysis revealed that thiamine

thiazole synthase gene is closely related to *Hordeum vulgare* thiamine thiazole synthase (HvTHI2) and *Brachypodium distachyon* thiamine thiazole synthase (BdTHI2) (Figure 1a). Therefore, we named that gene as TaTHI2-7A, TaTHI2-7B and TaTHI2-7D. For convenience, TaTHI2-7A (GenBank accession no. XM_044567543.1) was selected for further study and abbreviated as TaTHI2. In order to further confirm the function of TaTHI2, TaTHI2 was tested for complementation of yeast mutant strain. Firstly, we obtained a thiamine-deficient yeast strain through the knock-out thiamine thiazole synthase gene *THI4* in yeast strain (BY4741) using CRISPR-Cas9. Then, TaTHI2 was cloned into an expression vector of *S. cerevisiae* (pYES2) and introduced into the *thi4* knock-out mutant strain (Δ *thi4*) for functional complementation. The result showed that Δ *thi4* transformed with the empty plasmid barely grew in medium lacking thiamine, whereas Δ *thi4* expressing TaTHI2 grew as well as the wild type (BY4741) (Figure 1b). In a medium supplemented with thiamine, both strains grew well (Figure 1b). The results indicated that the expression of TaTHI2 can functionally complement the *THI4* knock-out mutant strain of *S. cerevisiae*, suggesting that TaTHI2 should have a similar function to *THI4* in thiamine biosynthesis. The subcellular localization of TaTHI2 was also investigated due to the presence of a chloroplast-targeting sequence (cTP) (TargetP-2.0) and its similarity to AtTHI1, which is known to be localized in chloroplasts and mitochondria (Chabregas et al., 2001). To determine the localization of TaTHI2, we expressed TaTHI2 fused with green fluorescent protein (GFP) driven by its native promoter (~2 kb upstream region) (pTHI2:TaTHI2-GFP) at 15 °C. A non-fused GFP (pTHI2:GFP) was used as a control. Confocal microscopy was performed to monitor GFP fluorescence. As expected, the expression of pTHI2:TaTHI2-GFP was observed in chloroplasts, while pTHI2:GFP was detected in the cytoplasm and nucleus in wheat protoplasts (Figure 1c).

The accumulation of membrane-localized TaTHI2 were increased in CWMV infection

To investigate the relationship between TaTHI2 and CWMV, we tested whether CWMV affects the subcellular localization of TaTHI2. Therefore, we expressed pTHI2:TaTHI2-GFP or co-expressed pTHI2:TaTHI2-GFP with CWMV in *N. benthamiana* leaves using agroinfiltration at 15 °C and observed the localization of TaTHI2 by confocal microscopy at 3–9 days. The results showed that pTHI2:TaTHI2-GFP was only observed in chloroplasts from 3 to 9 days post-inoculation in *N. benthamiana* leaves at 15 °C (Figure 2a). However, the accumulation level of non-chloroplast-localized TaTHI2 was increased from 3 to 9 days post-inoculation in *N. benthamiana* leaves infected with CWMV (Figure 2b). Previous studies have reported that THI1 in Arabidopsis is deposited at the plasma membrane when plants are treated with ABA (Li et al., 2016). Based on this, we hypothesized that TaTHI1 may be localized at the chloroplast and the plasma membrane during CWMV infection. To test this hypothesis, we used a subcellular fraction assay to analyse the localization of TaTHI2 at 3–9 days after CWMV infection. Western blot analysis showed that TaTHI2 was indeed localized in the plasma membrane and the chloroplast. Moreover, the accumulation level of membrane-localized TaTHI2 was increased in association with increases in CWMV CP (Figure 2c,d). To further confirm the localization of TaTHI2, we co-expressed plasma membrane intrinsic protein 2A (PIP2A)-RFP (RFP fused to the C-terminus of PIP2A) with pTHI2:TaTHI2-GFP plus CWMV

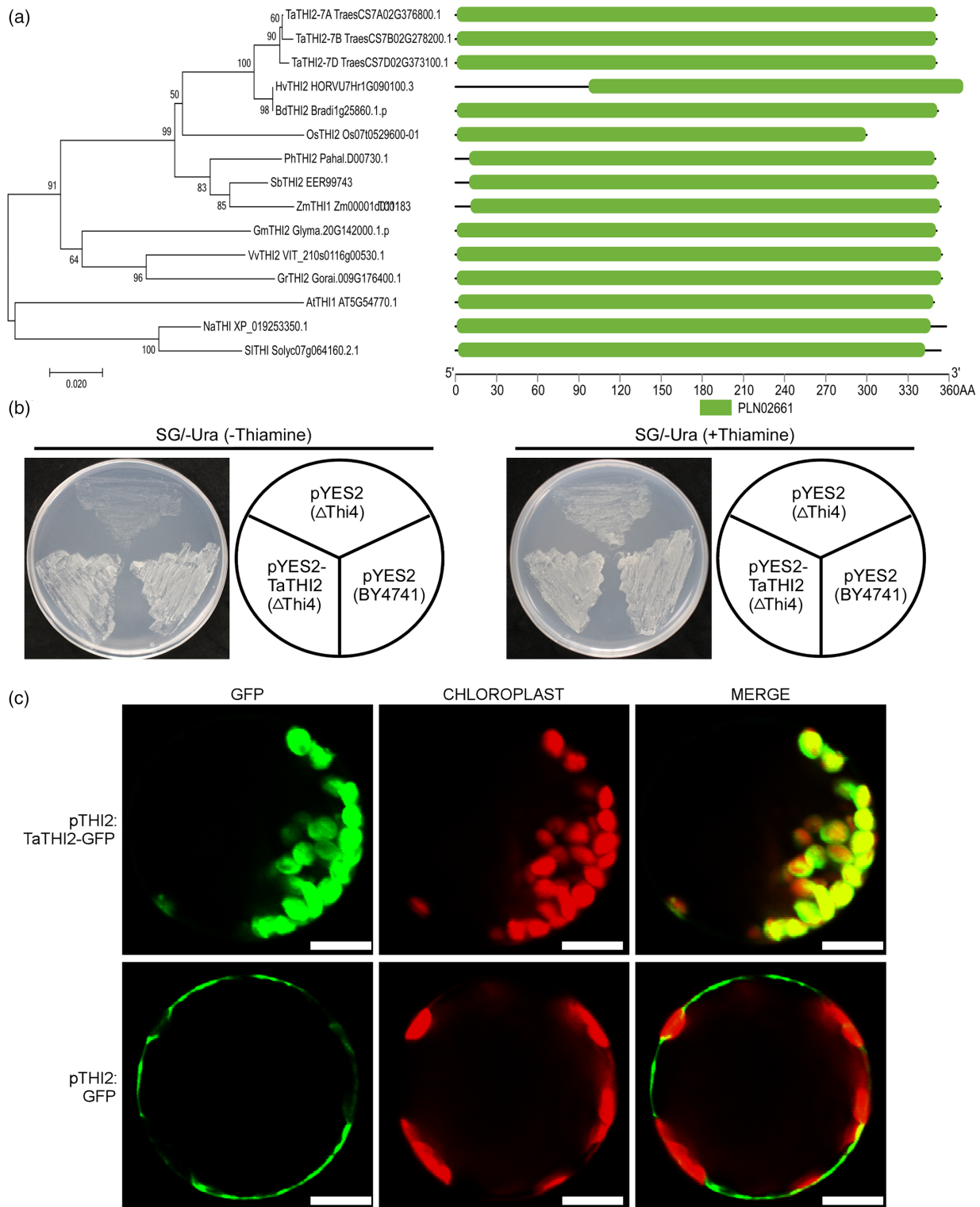


Figure 1 Characterization of TaTHI2 protein. (a) Phylogenetic and conserved domain analysis of THI4 from different plant species. The GenBank accession numbers and protein names are shown in branches. Sb, *Sorghum bicolor*; Zm, *Zea mays*; Ph, *Panicum hallii*; Os, *Oryza sativa*; Bd, *Brachypodium distachyon*; Hv, *Hordeum vulgare*; Ta, *T. aestivum*; Gm, *Glycine max*; Vv, *Vitis vinifera*; Gr, *Gossypium raimondii*; At, *Arabidopsis thaliana*; Na, *Nicotiana attenuata*; Sl, *Solanum lycopersicum*. (b) Functional complementation of the *S. cerevisiae* *thi4* mutant strain BY4741 with TaTHI2. The *thi4*-mutant strain was transformed with pYES2-TaTHI2, and the transformed cells were on the SG/-Ura medium without thiamine (left) and with 50 mg/L thiamine (right). The mutant strain transformed with the plasmid pYES2 was used as a negative control. BY4741 transformed with the plasmid pYES2 was used as a positive control. The yeast cells were grown on SG/-Ura plates at 30 °C for 3 days. (c) Subcellular localization of TaTHI2 protein in wheat protoplasts. TaTHI2 protein fused to green fluorescent protein under the control of the *TaTHI2* native promoter (pTHI2:TaTHI2-GFP) at 15 °C, and free GFP under the control of *TaTHI2* native promoter (pTHI2:GFP) was expressed in wheat protoplasts. Green fluorescence was observed under a confocal microscope. Bar: 10 μm.

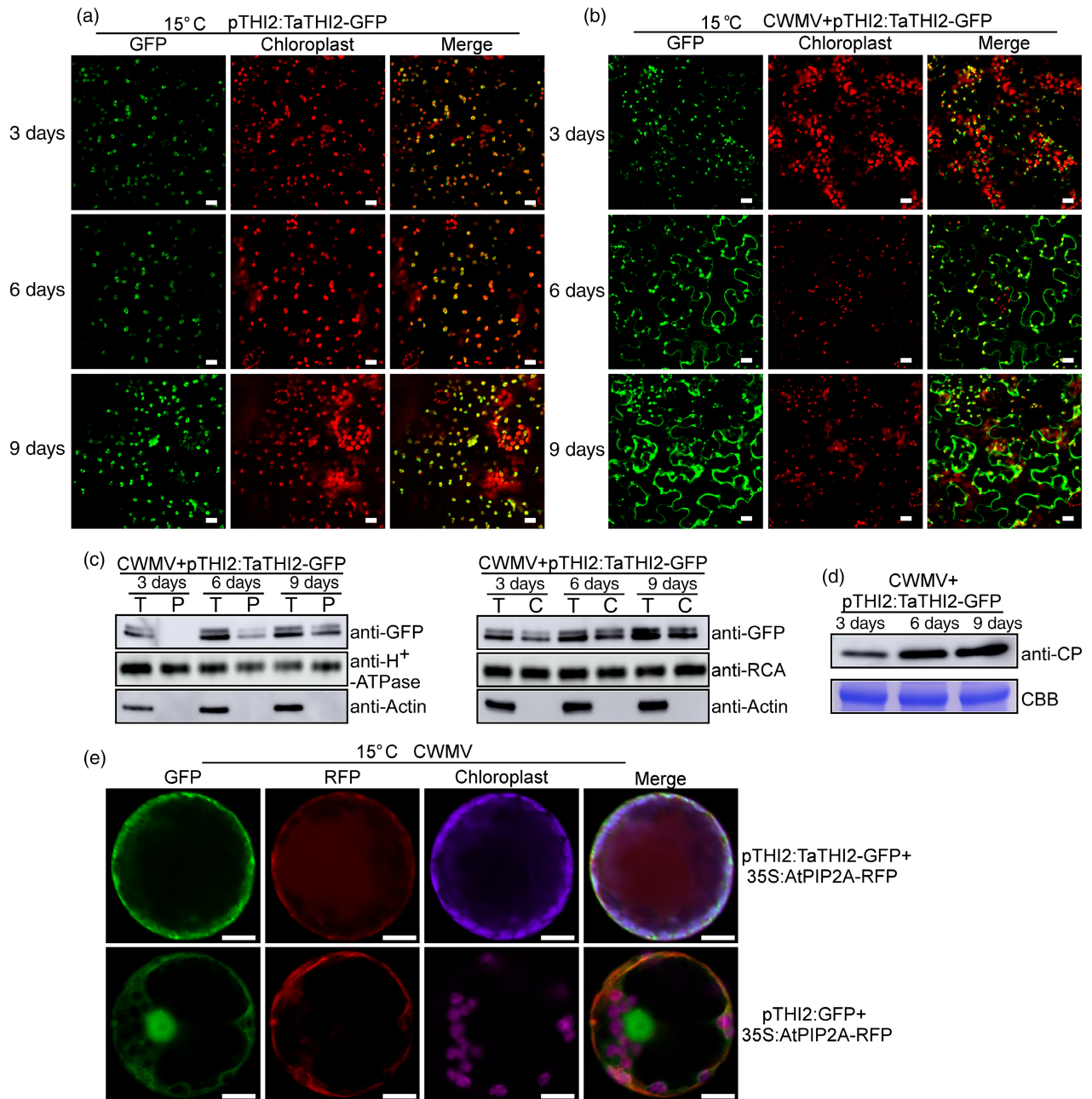


Figure 2 CWMV directs TaTHI2 to the cytoplasmic membrane. (a) Subcellular localization of pTHI2:TaTHI2-GFP at 15 °C in *N. benthamiana* leaves. Bar: 20 µm. (b) Subcellular localization of pTHI2:TaTHI2-GFP at 15 °C in *N. benthamiana* leaves infected with CWMV at 3–9 days. Bar: 20 µm. (c) Subcellular fractionation of pTHI2:TaTHI2-GFP at different stages of CWMV infection was detected by WB analysis. The actin, H⁺-ATP and RCA were used as a cytoplasm marker, cytoplasmic membrane marker and chloroplast maker. T (total protein); C (chloroplast); P (cytoplasmic membrane). (d) The accumulation of CWMV CP in the assayed *N. benthamiana* leaves was analysed by Western blot using a CWMV CP-specific antibody. (e) Colocalization of pTHI2:TaTHI2-GFP with PIP2A-RFP at 15 °C in wheat protoplasts infected with CWMV. pTHI2:GFP was co-expressed with PIP2A-RFP and was used as a control. Green or red fluorescence was observed under a confocal microscope. Bar: 10 µm.

(pTHI2:TaTHI2-GFP+PIP2A-RFP+CWMV) in wheat protoplasts and *N. benthamiana* leaves at 15 °C. PIP2A protein is used as a marker for membrane-localization (Marmagne *et al.*, 2004). Wheat protoplasts and *N. benthamiana* leaves expressing pTHI2:GFP plus CWMV and PIP2A-RFP (pTHI2:GFP+PIP2A-RFP+CWMV) were used as negative controls. Localization was observed via confocal microscopy. We found that the pTHI2:TaTHI2-GFP

product co-localized with both chloroplast and PIP2A-RFP, while pTHI2:GFP could not co-localize with chloroplast or PIP2A-RFP (Figures 2e and 52a). Next, total protein was extracted from *N. benthamiana* leaves expressing pTHI2:TaTHI2-GFP+PIP2A-RFP+CWMV and pTHI2:GFP+PIP2A-RFP+CWMV, respectively, and centrifuged to removed nuclei and large cellular debris at 3000 g. And then the supernatant was isolated into supernatant

fractions (S, soluble) and the microsomal fractions pellet (P, membrane-rich) fractions via high-speed centrifugation. Western blot analysis showed that GFP was present only in the S fraction, and PIP2A-RFP was detected in P (Figure S2b). However, pTHI2:TaTHI2-GFP was not only present in the P fraction but was also detected in the S fraction (Figure S2b). Furthermore, pTHI2:TaTHI2-GFP protein was detected when chloroplast protein was extracted separately (Figure S2c). Taken together these results indicate that TaTHI2 is deposited at plasma membrane under CWMV infection.

TaTHI2 positively contributes to CWMV resistance in wheat

To investigate the role of TaTHI2 in CWMV infection in wheat, we generated transgenic *TaTHI2*-RNAi plants on background YM158 by transgenic expressing hairpin RNAs with a segment of the conserved region of TaTHI2. The qRT-PCR result showed that *TaTHI2* was silenced in *TaTHI2*-RNAi plants (Figure S3). Next, *TaTHI2*-RNAi T1 generation and YM158 were inoculated with CWMV. After 21 dpi, *TaTHI2*-RNAi plants exhibited stronger mosaic symptoms than those of YM158 plants (Figure 3a). The qRT-PCR and Western blot results also showed higher accumulation levels of viral mRNA and protein in *TaTHI2*-RNAi lines compared to those in YM158 (Figure 3b,c). Furthermore, we silenced TaTHI2 using Barley stripe mosaic virus (BSMV) and observed a significant reduction in *TaTHI2* mRNA levels in BSMV:TaTHI2 infected plants compared to BSMV:00 infected plants (Figure S4a). The expression level of *TaTHI2-7B* and *TaTHI2-7D* in the BSMV:TaTHI2-infected plants compared to BSMV:00-infected plants was also decreased (Figure S4b). Next, we inoculated BSMV:TaTHI2+CWMV or BSMV:00+CWMV into wheat seedlings and found that plants infected with BSMV:TaTHI2+CWMV exhibited stronger mosaic symptoms than the control group of BSMV:00+CWMV after 14 dpi (Figure S4c). The qRT-PCR and Western blot results also showed higher accumulation levels of CWMV CP RNA and protein in plants inoculated with BSMV:TaTHI2+CWMV compared to the control group of BSMV:00+CWMV (Figure S4d,e).

To further investigate the role of TaTHI2, we overexpressed *TaTHI2* by transforming the TaTHI2-expression vector pTHI2:TaTHI2-His into wheat using the *Agrobacterium tumefaciens*-mediated method. We obtained three overexpression TaTHI2 transgenic lines (TH-L9, TH-L6 and TH-L2), and Western blot analysis confirmed the successful expression of TaTHI2 in these lines (Figure S5). Field nursery analysis of these transgenic lines in 2022 with a history of CWMV infection showed that they exhibited milder CWMV disease symptoms compared to the wild-type (WT) plants (Figure 3d). qRT-PCR and Western blot revealed lower accumulation levels of CWMV CP RNA and protein in these three lines compared to WT plants (Figure 3e,f). In addition, these three transgenic lines exhibited longer spike length compared to the 'YM158' plants when grown in a CWMV-contaminated nursery (Figure 3g,h), and their seed number per ear and 1000-kernel weight were also greater than 'YM158' plants (Figure 3i). The incidence of TH-L9, TH-L6 and TH-L2 plants after CWMV infection was also significantly decreased (Figure 3j,k). Furthermore, *TaTHI2-OE* plants and YM158 were inoculated with BSMV, respectively. The result showed that *TaTHI2-OE* plants and YM158 exhibit similar mosaic symptoms after inoculated with BSMV (Figure S6a). The qRT-PCR results also showed that the accumulation level of viral mRNA has no significant changes in *TaTHI2-OE* plants compared to that in YM158 (Figure S6b).

Moreover, we analysed the agronomic traits and thiamine content of six *TaTHI2-OE* transgenic lines (TH-L9, TH-L6, TH-L2, TH-L5, TH-L8, TH-L1) grown in a CWMV-contaminated nursery in 2023. The results showed that the seed number per ear was up-regulated by 40%, 44.4%, 40%, 37.8%, 28.9%, 15.6% and 1000-kernel weight was up-regulated by 18.9%, 14.7%, 16.8%, 15.2%, 7.9%, 5.1%, respectively, in these six *TaTHI2-OE* transgenic lines compared to YM158 (Figure 3l). The thiamine content of these six *TaTHI2-OE* transgenic lines was up-regulated by 55%, 52.8%, 52%, 45%, 17.5%, 14.4%, respectively, compared to YM158 (Figure 3m). In addition, Western blot analysis revealed that the protein accumulation level of TaTHI2 is positively correlated with wheat seed number per ear and 1000-kernel weight (Figure 3n). Moreover, multiple key agronomic yield traits of these *TaTHI2-OE* transgenic lines were evaluated when grown in a CWMV-contaminated nursery, and the results showed significant increases in the spike length, spike width, grain length and grain width compared to YM158 plants (Figure S7). Based on these results, it can be found that there is a potential positive relationship between the yield of the transgenic lines and thiamine content. In summary, these results indicate that TaTHI2 positively contributes to CWMV resistance in wheat and that *TaTHI2-OE* wheat plants may improve yield by increasing thiamine content.

TaTHI2 interacts with TaCPK5 and represses its kinase activity

To explore the molecular mechanism of TaTHI2 in the regulation of CWMV infection, we identified TaTHI2-interacting proteins using liquid chromatography tandem mass spectrometry (LC-MS/MS). Initially, we detected TaTHI2 in the total protein extracted from wheat leaf protoplasts transiently expressing pTHI2:TaTHI2-GFP and CWMV. Immunoprecipitation (IP) assays using anti-GFP agarose beads identified TraesCS2D02G229100.1 (named TaCPK5) as the highest confidence interacting protein (Table S1). TaCPK5 contains a kinase domain (KD) and has a length of 532 amino acids. Co-immunoprecipitation (Co-IP) and complementation imaging (LCI) assays confirmed the interaction between TaTHI2 and TaCPK5 (Figure 4a,b). To determine the localization of the interaction, TaCPK5 fused to a red fluorescent protein (TaCPK5-RFP) was co-expressed with pTHI2:TaTHI2-GFP in wheat protoplast and *N. benthamiana* leaves at 15 °C, respectively. We observed colocalization of the pTHI2:TaTHI2-GFP product and TaCPK5-RFP in the plasma membrane using confocal microscopy (Figures 4c and S8a). Subsequently, we extracted total protein from *N. benthamiana* leaves expressing pTHI2:TaTHI2-GFP and TaCPK5-RFP and isolated them into P and S fractions via high-speed centrifugation. Western blot analysis showed that pTHI2:TaTHI2-GFP and TaCPK5-RFP were co-detected in the extracted total protein as well as in the P fraction protein (Figure S8b), suggesting that TaTHI2 and TaCPK5 are co-localized in the plasma membrane. According to the above results, we hypothesized that TaTHI2 is a substrate of TaCPK5 and therefore performed an *in vitro* phosphorylation assay. Both TaCPK5-GST and TaTHI2-His were expressed and purified from *E. coli*. The result showed that TaCPK5 did not phosphorylate TaTHI2, but the autophosphorylation activity was inhibited in the presence of TaTHI2 (Figure 4d). In addition, no significant difference in the expression level of *TaCPK5* between *TaTHI2-OE* transgenic wheat plants and YM158 plants (Figure S9). Based on this, we hypothesize that the interaction between TaTHI2 and TaCPK5 may interfere with the autophosphorylation of TaCPK5.

To test this possibility, we conducted a series of kinase assays of TaCPK5-GST in the presence of different concentrations of TaTHI2-His *in vitro*. Our results showed that TaTHI2 reduced the pIMAGO signal of TaCPK5 in a dose-dependent manner, indicating that TaCPK5 had autophosphorylation activity and that the autophosphorylation activity of TaCPK5 was repressed by TaTHI2 (Figure 4e).

TaTHI2 represses the TaCPK5-enacted phosphorylation of TaCAT1

To investigate whether TaTHI2 can modulate the kinase activity of TaCPK5, we sought to identify TaCPK5-interacting proteins. TaCPK5-GFP was transiently expressed in wheat leaf protoplasts and immunoprecipitated after 48 h. The immunoprecipitation

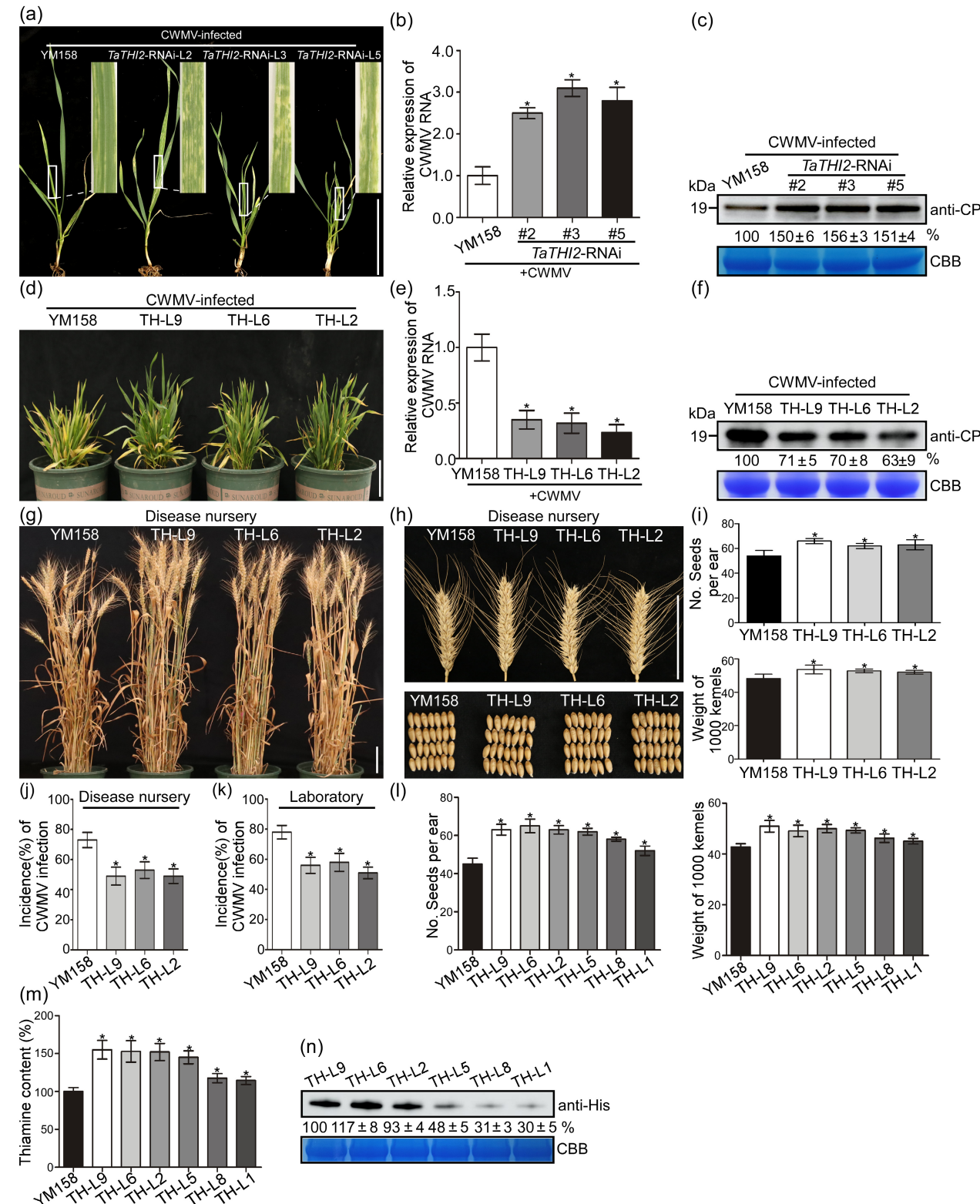


Figure 3 TaTHI2 positively regulated CWMV infection. (a) Phenotypes after 21 dpi of *TaTHI2*-RNAi plants inoculated with CWMV. # 2, 3, 5 represent three independent lines of *TaTHI2*-RNAi. (b) The accumulation of CWMV CP in *TaTHI2*-RNAi and YM158 plants was analysed by qRT-PCR. YM158 was used as the control. (c) CWMV accumulation in *TaTHI2*-RNAi and YM158 plants was detected by Western blot using a CWMV CP-specific antibody. (d) Assessment of *TaTHI2* transgenic lines (TH-L9, TH-L6 and TH-L2) plants for disease resistance in a virus-contaminated nursery at Rongcheng, Shandong Province in 2022. YM158, which is susceptible to CWMV, was used as the negative control. (e) The accumulation of CWMV CP in TH-L9, TH-L6, TH-L2 and YM158 plants in field were analysed by qRT-PCR. YM158 was used as the control. (f) CWMV accumulation in TH-L9, TH-L6, TH-L2 and YM158 plants in field was detected by Western blot using a CWMV CP specific antibody. (g) Phenotypes of YM158, TH-L9, TH-L6, TH-L2 plants at maturity. (h) Comparison of seed health and wheat ears among transgenic plants and YM158 in the disease field. (i) Analysis of seed number per wheat ear and 1000-kernel weight of the TH-L9, TH-L6, TH-L2 and YM158 plants at maturity. (j) CWMV incidence in YM158 and TH-L9, TH-L6, TH-L2 plants in field. (k) CWMV incidence in YM158 and TH-L9, TH-L6, TH-L2 plants in laboratory. Mean \pm SD values are from three independent experiments with 45 plants per treatment. (l) Analysis of seed number per wheat ear and 1000-kernel weight of the TH-L9, TH-L6, TH-L2, TH-L5, TH-L8, TH-L1 and YM158 plants at maturity in the disease field. (m) Total thiamine contents in the YM158 and *TaTHI2*-OE transgenic lines were measured using HPLC. (n) The *TaTHI2* protein accumulation level in *TaTHI2*-OE plants was analysed through western blot analysis using an anti-His antibody. Coomassie brilliant blue (CBB) served as loading controls. Statistical analysis was performed using Student's *t*-test. **P* < 0.05. Bar: 10 cm.

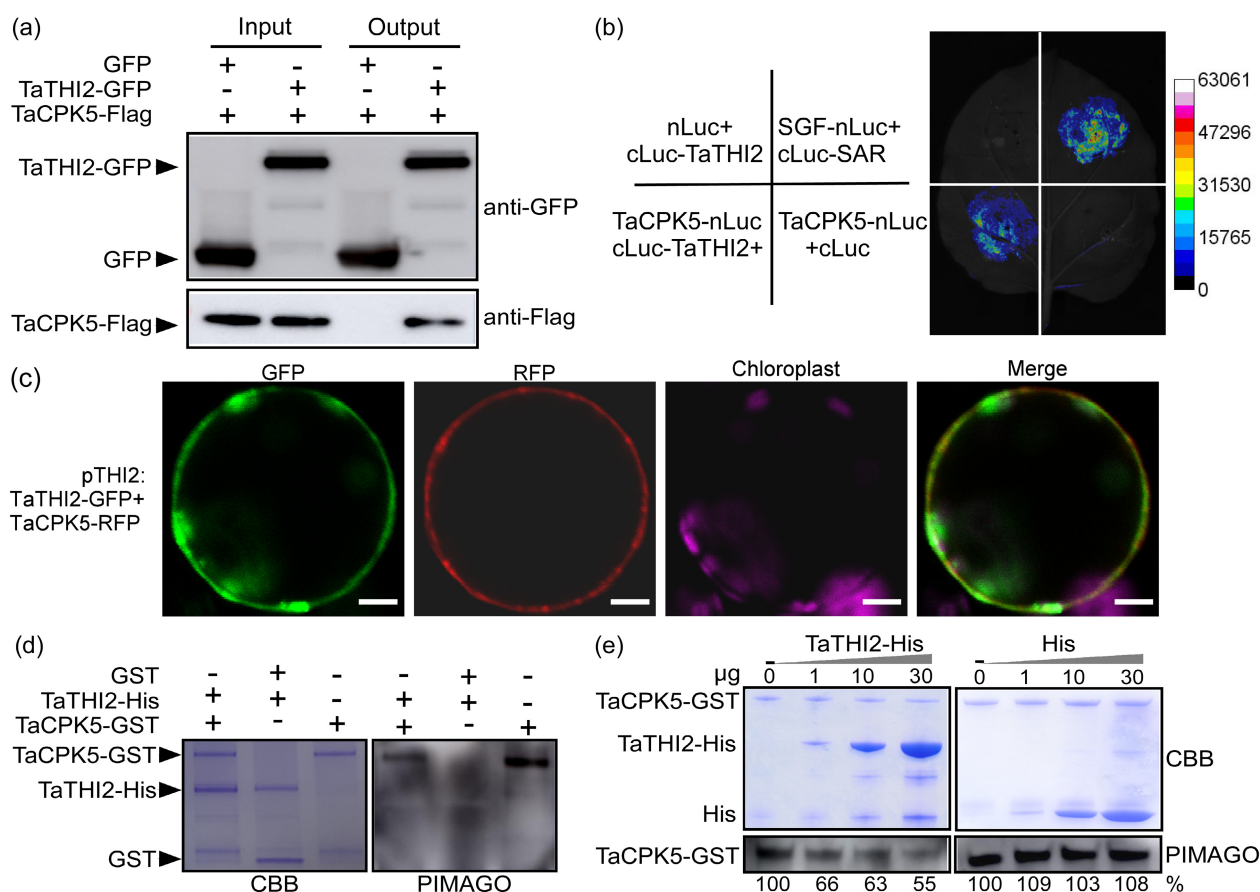


Figure 4 TaTHI2 interacts with TaCPK5 and represses its autophosphorylation activity. (a) CO-IP analysis for interaction between TaTHI2 with TaCPK5 *in vivo*. TaTHI2-GFP and TaCPK5-Flag were co-expressed in *N. benthamiana* leaves, and total protein was immunoprecipitations with anti-GFP beads. Protein samples and IP products were detected in Western blots with anti-GFP or anti-Flag antibodies. (b) Luciferase complementation imaging (LCI) assay was used to confirm the interaction between TaTHI2 and TaCPK5 in *N. benthamiana* leaves. The leaf areas infiltrated with *Agrobacterium* cultures expressing SGF-nLuc+cLuc-SAR were used as the positive controls, nLuc+cLuc-TaTHI2 and TaCPK5-nLuc+cLuc were used as the negative controls, respectively. Luciferase activity was captured using a low-light cooled CCD imaging apparatus at 3 days. (c) Colocalization of pTHI2:TaTHI2-GFP with TaCPK5-RFP at 15 °C in wheat protoplasts. Green or red fluorescence was observed under a confocal microscope. Bar, 10 µm. (d) Phosphorylation of TaTHI2-His by TaCPK5-GST was detected *in vitro*. TaTHI2-His+GST and TaCPK5-GST were used as the negative controls. Left: SDS-PAGE separation of purified TaTHI2-His, TaCPK5-GST and His. Right: Blots were probed with pIMAGO for the detection of phosphoproteins. (e) Autophosphorylation activity of TaCPK5-GST in the presence of increasing concentrations of TaTHI2-His protein (0, 1, 10 and 30 µg; indicated by the triangle) or His control. Top: SDS-PAGE separation of purified proteins. Bottom: The autophosphorylation of TaCPK5-GST in the presence of TaTHI2-His and His *in vitro*.

samples were then subjected to LC-MS to identify potential interacting proteins. Among them, TraesCS4B02G325800.1, named TaCAT1, showed the highest confidence and was chosen

for further analysis. Co-IP and LCI assays confirmed the interaction between TaCPK5 and TaCAT1 (Figure 5a,b), suggesting that TaCAT1 might be a substrate of TaCPK5. To test this

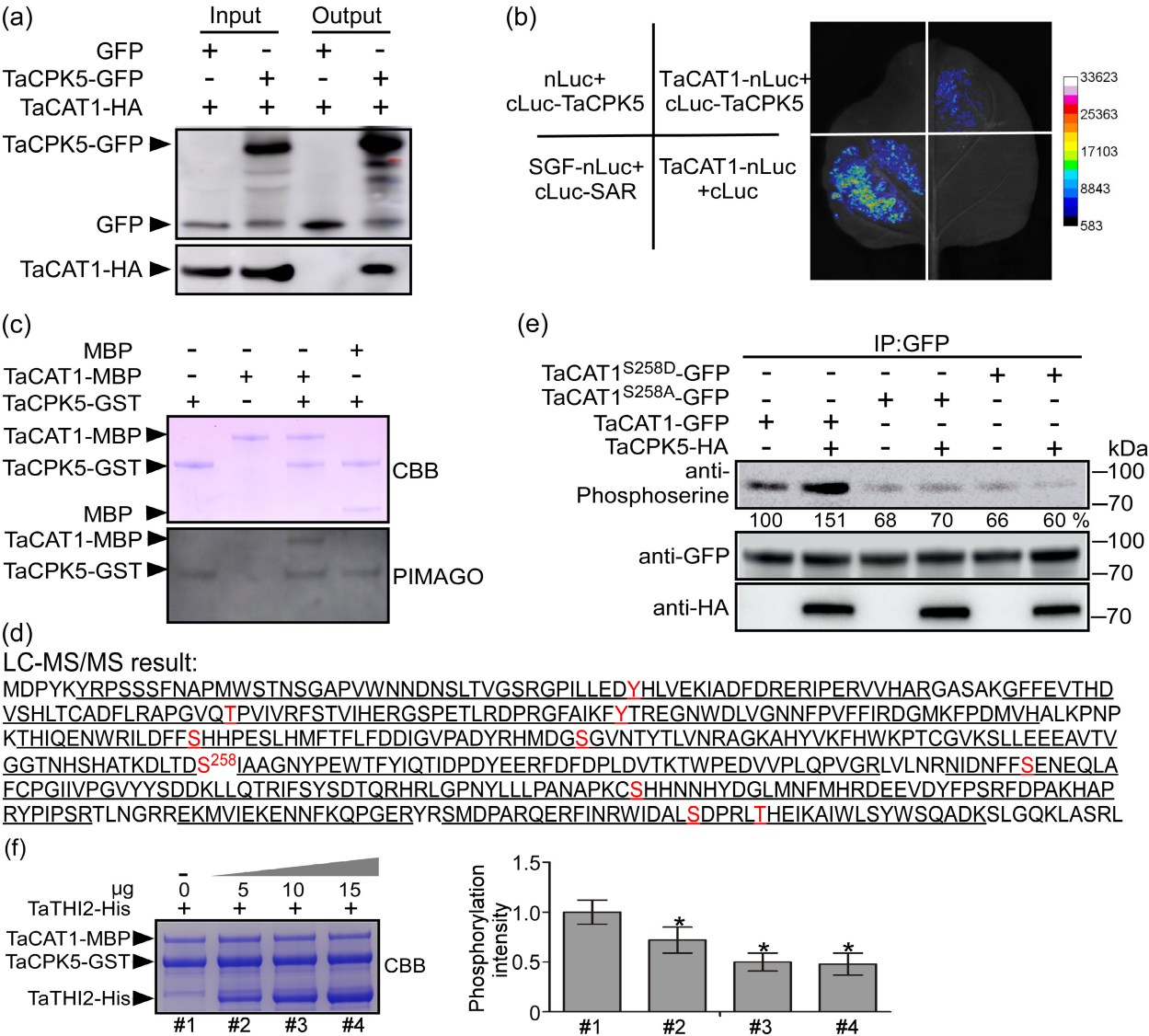


Figure 5 TaTHI2 affects the ability of TaCPK5 to phosphorylate TaCAT1. (a) CO-IP analysis for interaction between TaCPK5 with TaCAT1 *in vivo*. TaCPK5-GFP and TaCAT1-HA were co-expressed in *N. benthamiana* leaves and total protein were immunoprecipitations with anti-GFP beads at 3 dpi. Protein samples and IP products were detected in Western blots with anti-GFP or anti-HA antibodies. (b) LCI assay was used to confirm the interaction between TaCPK5 and TaCAT1. (c) Phosphorylation of TaCAT1-MBP by TaCPK5-GST was detected *in vitro*. TaCPK5-GST+MBP were used as the negative controls. Top: SDS-PAGE separation of purified TaCAT1-MBP, TaCPK5-GST and MBP. Bottom: Blots were probed with pIMAGO for the detection of phosphoproteins. (d) LC-MS/MS assay was used to detect the potential phosphorylation sites in TaCAT1. The underlined TaCAT1 amino acid sequence was identified in this study through LC-MS/MS, and the phosphorylation sites in this protein are shown in red. (e) The phosphorylation of TaCAT1-GFP, TaCAT1^{S258A}-GFP and TaCAT1^{S258D}-GFP was determined in the presence of TaCPK5-HA protein through Western blot using a phosphoserine-specific antibody. Total proteins were used to detect accumulation of TaCAT1, TaCAT1^{S258A}, TaCAT1^{S258D} and TaCPK5 in Western blots with anti-GFP and HA antibodies, respectively. (f) Quantification of phosphorylation TaCAT1-MBP at S258 in the presence of TaCPK5-GST and increasing concentrations of TaTHI2-His protein (0, 1, 10 and 30 µg; # 1, 2, 3, 4 represent above experimental groups). Left: SDS-PAGE separation of purified TaTHI2-His, TaCPK5-GST and TaCAT1-MBP. Right: The phosphorylation level of TaCAT1 at S258 in the above experimental groups (# 1, 2, 3, 4). The phosphorylated peptides were identified through LC-MS/MS using the PRM method. Peptide phosphorylation ratios (e.g. phosphorylated/non-phosphorylated) were then determined. The data presented are the means ± SD, determined using the Student's *t*-test. Each treatment had three technical replicates. **P* < 0.05.

possibility, purified TaCAT1-MBP was incubated with TaCPK5-GST in kinase buffer *in vitro*, and the phosphorylation status of TaCAT1 was assessed using the pIMAGO kit. Figure 5c shows that TaCAT1 was indeed phosphorylated by TaCPK5. To identify the phosphorylation site in TaCAT1, we performed LC-MS/MS analysis on six independent samples. Based on the results, we identified 10 potential phosphorylation sites in TaCAT1 (Figure 5d). Among them, Ser-258 was identified in three

independent assays and was thus selected for further investigation (Table S2). To further verify whether Ser-258 is the phosphorylation site in TaCAT1 by TaCPK5, we generated a plasmid expressing a TaCAT1-GFP fusion with Ser-258 mutated to Ala (TaCAT1^{S258A}-GFP). We also generated a plasmid expressing a TaCAT1-GFP fusion with Ser-258 mutated to Asp (TaCAT1^{S258D}-GFP). We then performed an *in vivo* kinase assay by co-expressing TaCAT1-GFP, TaCAT1^{S258A}-GFP, TaCAT1^{S258D}-GFP

or both with TaCPK5-HA in *N. benthamiana* leaves. At 3dpi, total proteins were extracted and immunoprecipitated with anti-GFP beads, and the phosphorylation status was analysed by Western blotting with anti-phosphoserine antibodies. We observed that the phosphorylation level of TaCAT1 was increased when co-expressed with TaCPK5, whereas TaCPK5 had no effect on the phosphorylation level of TaCAT1^{S258A} and TaCAT1^{S258D}, which was decreased compared to TaCAT1 (Figure 5e). To investigate whether TaTHI2 regulates the TaCPK5-mediated phosphorylation of TaCAT1 at S258, we conducted a series of kinase assays. Increasing amounts of TaTHI2-His protein (0, 5, 10 and 15 µg) were added to the kinase buffer containing TaCPK5-GST and TaCAT1-MBP. The phosphorylation status of TaCAT1 at S258 was then determined by LC-MS/MS analysis using a parallel reaction monitoring (PRM) system. The results showed that the presence of TaTHI2 significantly reduced the phosphorylation of TaCAT1 at S258, indicating that TaTHI2 negatively regulates the TaCPK5-mediated phosphorylation of TaCAT1 at S258 (Figure 5f).

TaTHI2 promotes the accumulation of ROS by repressing the TaCPK5-enacted activity of TaCAT1

To investigate the significance of TaCAT1 phosphorylation by TaCPK5, we conducted a catalytic activity assay in the presence of TaCPK5. We found that TaCPK5 significantly enhanced TaCAT1 activity, while it did not influence the catalase activity of TaCAT1^{S258A} (Figure S10). To further elucidate the role of TaCPK5 in TaCAT1 catalase activity in plants, we analysed the accumulation level of ROS production after the transient expression of TaCAT1:GFP, TaCAT1^{S258A}:GFP, TaCAT1:GFP+TaCPK5:HA, TaCAT1^{S258A}:GFP+TaCPK5:HA or GFP (EV) in *N. benthamiana* leaves. At 2 dpi, CWMV was infiltrated into these leaves. ROS accumulation in these plants was analysed using diaminobenzidine tetrahydrochloride (DAB) staining and nitroblue tetrazolium (NBT) staining. The results showed that ROS accumulation was significantly reduced in *N. benthamiana* leaves expressing TaCAT1:GFP compared to the leaves expressing GFP, and the leaves co-expressing TaCAT1:GFP+TaCPK5:HA accumulated even lower ROS production than TaCAT1:GFP (Figure 6a,b). Moreover, the leaves expressing TaCAT1^{S258A}:GFP accumulated a moderate level of ROS, and the level of ROS accumulation in leaves co-expressing TaCAT1^{S258A}:GFP+TaCPK5:HA was similar to that of TaCAT1^{S258A}:GFP (Figure 6a,b). These results demonstrate that TaCPK5 can reduce the accumulation of ROS by enhancing TaCAT1 activity and indicate again that Ser-258 is the key site of TaCAT1 that is phosphorylated by TaCPK5. Then, in order to investigate whether TaTHI2 affects the accumulation of ROS production mediated by TaCPK5-TaCAT1, we constructed C-terminal HA-tagged TaCPK5 (TaCPK5-HA) and C-terminal Flag-tagged TaCAT1 (TaCAT1-flag) recombinant plasmids. We conducted six different experimental groups (I–VI) to assess the content of ROS production. Plants in Group I were taken as the positive control. DAB staining and NBT staining showed that ROS accumulation increased in a dose-dependent manner with increasing concentration of TaTHI2 in TaCAT1-flag+TaCPK5-HA overexpressed leaves (Figure 6c,d). In addition, there was no significant change in the content of ROS production in a dose-dependent manner with increasing concentration of GFP in TaCAT1-flag +TaCPK5-HA overexpressed leaves (Figure S11). Furthermore, we also analysed the accumulation of ROS production in TaTHI2 transgenic plants during CWMV infection. Wheat samples were stained with DAB and NBT. YM158 was used as a control. ROS accumulation was significantly increased in

TH-L9, TH-L6 and TH-L2 plants compared to control plants (Figure 6e,f). In conclusion, these results demonstrate that TaTHI2 promotes ROS accumulation by interrupting the TaCPK5-enacted TaCAT1 catalase activity, leading to increased ROS accumulation.

CWMV CP resumes the kinase activity of TaCPK5 through competitively binds to TaTHI2

To establish a successful infection, viral proteins can directly interact with plant proteins. We speculated whether viral proteins could also interact with TaTHI2. Therefore, we used TaTHI2 as bait to screen a CWMV cDNA library by yeast two-hybrid (Y2H) assay. CWMV coat protein (CP) showed a strong interaction with TaTHI2. Further Y2H assays confirmed the strong and specific interaction between CWMV CP and TaTHI2 (Figure 7a). LCI experiments also supported the interaction between CWMV CP and TaTHI2 (Figure 7b). In addition, we inspected the subcellular localization of TaTHI2 when co-expressed with 35S:CP-RFP (RFP fused to its C-terminus) in wheat protoplast and *N. benthamiana* leaves at 15 °C by confocal microscopy, respectively. We found that the pTHI2:TaTHI2-GFP product colocalized with CP-RFP in cells (Figures 7c and S12a). We then extracted total protein from the *N. benthamiana* leaves expressing pTHI2:TaTHI2-GFP and CP-RFP and isolated it into P and S fractions by high-speed centrifugation. Western blot analysis showed that pTHI2:TaTHI2-GFP and CP-RFP were co-detected in the extracted total protein, S, and P fraction protein (Figure S12b). These results suggest that TaTHI2 and CP can co-localize at the plasma membrane. Considering that both TaCPK5 and CP can interact with TaTHI2, we wondered whether CP could interfere with TaTHI2-TaCPK5 interactions. To explore this hypothesis, a pull-down assay of TaTHI2 and TaCPK5 in the presence of different concentrations of CP was used. We observed that the increase of CP-MBP concentration gradually decreased the amount of TaCPK5-GST bound by TaTHI2-His. In contrast, the increase of MBP did not influence the interaction of TaTHI2 with TaCPK5 (Figure 7d). These results suggest that CWMV CP competes with TaCPK5 to bind to TaTHI2. Since TaTHI2 can repress the autophosphorylation activity of TaCPK5, it seems likely that CP can influence the autophosphorylation activity of TaCPK5 in the presence of TaTHI2. To investigate this possibility, we conducted a series of kinase assays. Based on our previous findings, we determined the optimal concentration of TaTHI2 to inhibit the autophosphorylation of TaCPK5 to be 10 µg (Figure 4e). We gradually increased the amount of CP-MBP protein (0, 1, 8, and 20 µg) in the kinase buffer containing TaCPK5-GST (1 µg) and TaTHI2-His (10 µg). We observed a dose-dependent increase in the pIMAGO signal as the amount of CP-MBP protein increased, indicating the resumption of autophosphorylation of TaCPK5 (Figure 7e). In contrast, the increase of MBP did not affect the pIMAGO signal (Figure 7e). These results suggest that CWMV CP disrupts the formation of the TaTHI2-TaCPK5 complex and promotes the autophosphorylation of TaCPK5.

CWMV CP negatively regulates ROS accumulation and promotes CWMV infection

To investigate the role of CWMV CP in virus infection, we introduced the CWMV CP-expression vector pWMB190-CP into wheat using the *Agrobacterium tumefaciens*-mediated method, resulting in three transgenic lines expressing CWMV CP (T-L8, T-L6 and T-L1). The expression of CWMV CP in these lines was confirmed by RT-PCR (Figure S13). In a field nursery with a history of CWMV infection in 2022, we observed that the transgenic lines (T-L8, T-L6 and T-L1) showed stronger CWMV symptoms

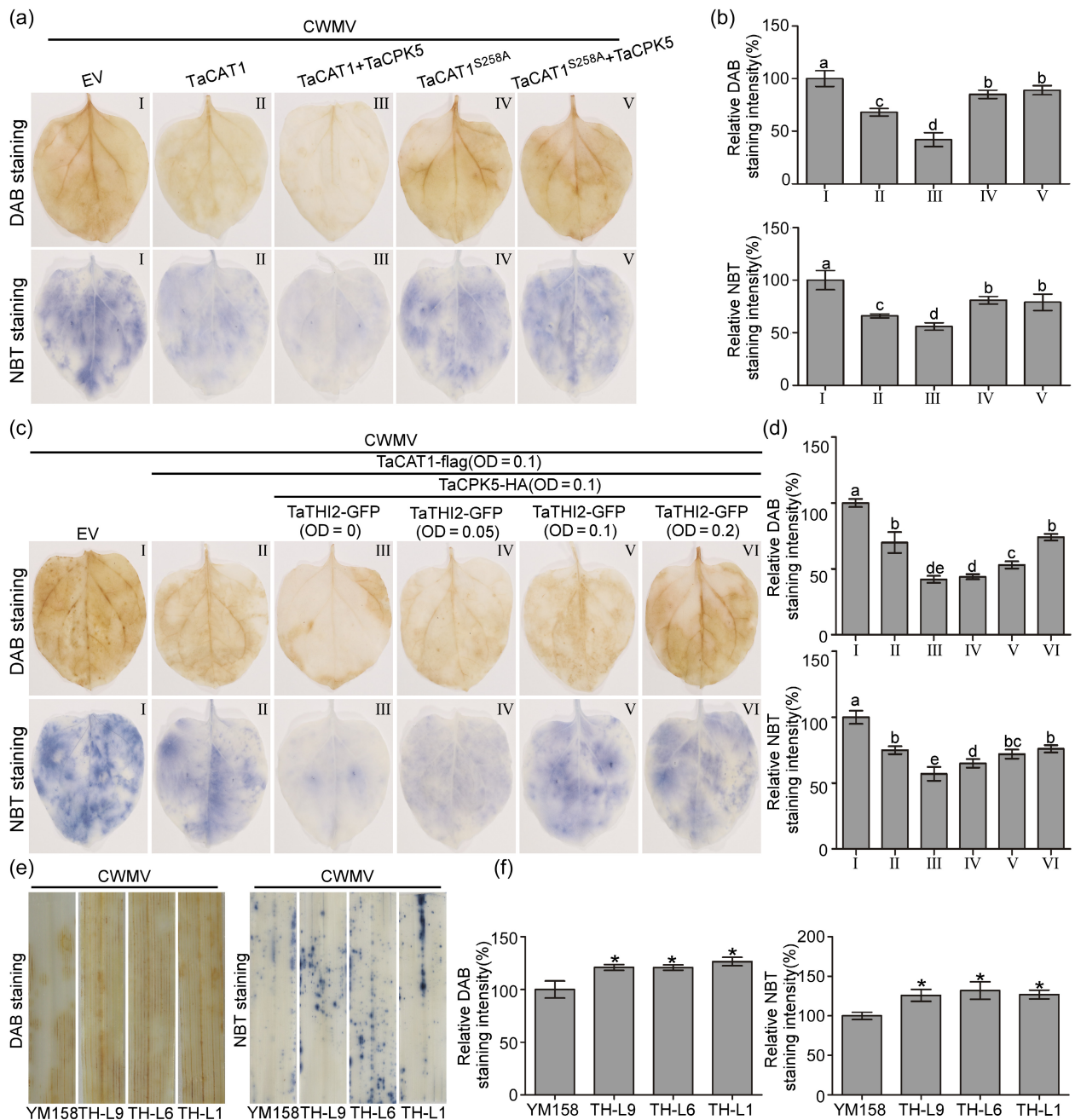


Figure 6 TaTHI2 regulates the TaCPK5-TaCAT1 module to promote the accumulation of H_2O_2 . (a) The *N. benthamiana* leaves inoculated with CWMV+GFP, CWMV + TaCAT1:GFP, CWMV + TaCAT1:GFP + TaCPK5:HA, CWMV + TaCAT1^{S258A}:GFP, CWMV + TaCAT1^{S258A}:GFP + TaCPK5:HA, CWMV + GFP (EV) were used as control. The assayed leaves were stained with DAB and NBT solution to detect ROS production. (b) Measurement of the relative DAB and NBT staining intensity as shown in (a). Values were obtained by measuring three representative images chosen from three biological replicates, the data presented are the means \pm SD. Different letters show statistically significant differences ($P < 0.05$, Tukey's test). (c) A range of different treated *N. benthamiana* leaves (I–VI) which represent CWMV + EV (empty vector), CWMV + TaCAT1-flag (OD600 = 0.1), CWMV + TaCAT1-flag (OD600 = 0.1) + TaCPK5-HA (OD600 = 0.1), CWMV + TaCAT1-flag (OD600 = 0.1) + TaCPK5-HA (OD600 = 0.1) + TaTHI2-GFP (OD600 = 0.05), CWMV + TaCAT1-flag (OD600 = 0.1) + TaCPK5-HA (OD600 = 0.1) + TaTHI2-GFP (OD600 = 0.1), CWMV + TaCAT1-flag (OD600 = 0.1) + TaCPK5-HA (OD600 = 0.1) + TaTHI2-GFP (OD600 = 0.2) were stained with DAB and NBT solution to detect ROS production. (d) Measurement of the relative DAB and NBT staining intensity as shown in (c). Values were obtained by measuring three representative images chosen from three biological replicates, the data presented are the means \pm SD. Different letters show statistically significant differences ($P < 0.05$, Tukey's test). (e) ROS production in TH-L9, TH-L6, TH-L2 and YM158 plants infected with CWMV was analysis by DAB and NBT staining. YM158 was used as the control. (f) Measurement of the relative DAB and NBT staining intensity as shown in (e). Values were obtained by measuring three representative images chosen from three biological replicates, the data presented are the means \pm SD. Statistical analysis was performed using Student's *t*-test. * $P < 0.05$.

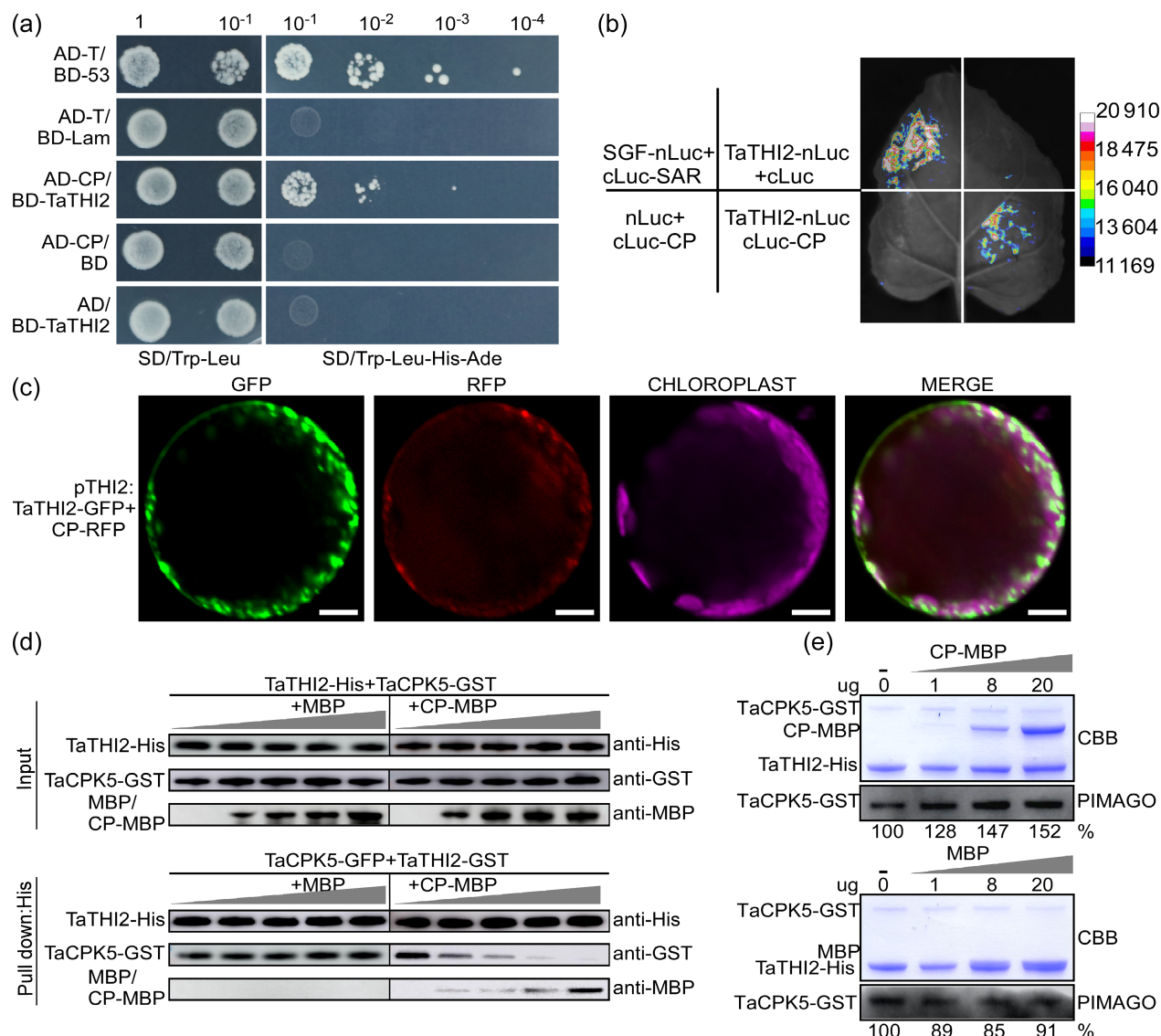


Figure 7 CWMV CP take TaTHI2 away from the TaTHI2-TaCPK5 subcomplex to resumes the kinase activity of TaCPK5. (a) Interaction of CWMV CP and TaTHI2 in yeast two-hybrid (YTH) assay. Yeast cells co-transformed with AD-CP and BD-TaTHI2, and the transformed cells were grown on the SD/-Leu/-Trp medium and then on the SD/-Trp/-Leu/-His/-Ade medium. Yeast cells co-transformed with AD-T/BD-Lam, AD-CP/BD and AD/BD-TaTHI2 were used as the negative controls, and yeast cells co-transformed with AD-T/BD-53 were used as the positive controls. (b) LCI assay was used to confirm the interaction between CWMV CP and TaTHI2. (c) Colocalization of pTHI2:TaTHI2-GFP with CP-RFP at 15 °C in wheat protoplasts. Green or red fluorescence was observed under a confocal microscope. Bar: 10 µm. (d) CWMV CP competes with TaCPK5 to bind TaTHI2 *in vitro* in a dose-dependent manner. Co-precipitation of TaCPK5-GST with TaTHI2-His in the presence of MBP or CP-MBP was detected by Western blot before (input) and after affinity purification (His pull-down). (e) CWMV CP resumes TaCPK5 autophosphorylation activity. TaCPK5-GST was incubated with TaTHI2-His and the increasing concentration of CP-MBP (0, 1, 8 and 20 µg; indicated by the triangle) or MBP (Maltose binding protein). Top: SDS-PAGE separation of purified proteins. Bottom: The autophosphorylation of TaCPK5-GST in the presence of CP-MBP and MBP *in vitro*.

than the control plants (Figure 8a). Further analysis using qRT-PCR and Western blot showed that the accumulation levels of CWMV RNA and CP protein in these three lines were significantly higher than in the control (Figure 8b,c). Moreover, when grown in a CWMV-contaminated nursery, the transgenic lines had shorter spike lengths compared to 'YM158' plants, and the seed number per ear and 1000-kernel weight of these lines were also less than 'YM158' plants (Figure 8d-f). These results indicate that CWMV CP facilitates CWMV infection in wheat. Since our study demonstrated that CWMV CP disrupts the formation of the TaTHI2-TaCPK5 complex and restores the kinase activity of

TaCPK5, we investigated whether CWMV CP can also regulate the accumulation of ROS. To test this hypothesis, we performed DAB and NBT assays to analyse ROS accumulation in three transgenic CWMV CP expressing wheat lines T-L8, T-L6 and T-L1 during CWMV infection, with YM158 serving as the control. The results of DAB and NBT staining showed a significant reduction in ROS accumulation in T-L8, T-L6 and T-L1 compared to the control (Figure 8g,h). In addition, the incidence of T-L8, T-L6 and T-L1 plants after CWMV infection was significantly increased (Figure 8i,j). Thus, these data suggest that CWMV CP facilitates CWMV infection by reducing ROS accumulation.

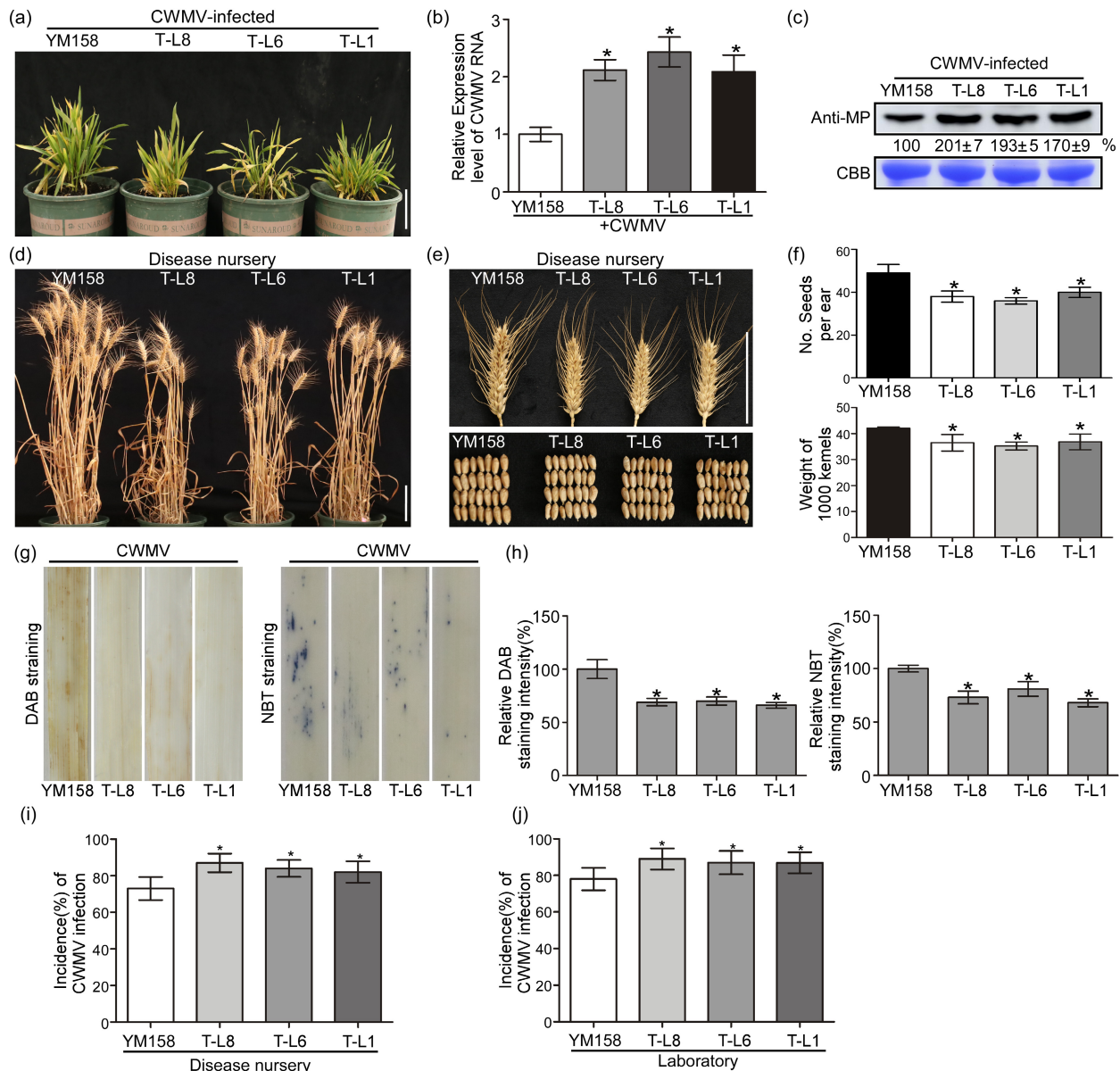


Figure 8 CWMV CP scavenges ROS promoting viral infection. (a) Assessment of CWMV CP transgenic lines (T-L8, T-L6 and T-L1) plants for disease resistance in a virus-contaminated nursery at Rongcheng, Shandong Province in 2022. YM158, which is susceptible to CWMV, was used as the negative control. (b) The accumulation of CWMV MP in T-L8, T-L6, T-L1 and YM158 plants in fields were analysed by qRT-PCR. YM158 was used as the control. The data presented are the means \pm SD, determined using the Student's *t*-test. Each treatment had three biological replicates. **P* < 0.05. (c) CWMV accumulation in T-L8, T-L6, T-L1 and YM158 plants in fields was detected by Western blot using a CWMV MP-specific antibody. (d) Phenotypes of YM158, T-L8, T-L6 and T-L1 plants at maturity. (e) Comparison of seed health and wheat ears among transgenic plants and YM158 in the disease field. (f) Analysis of seed number per wheat ear and 1000-kernel weight of the T-L8, T-L6, T-L1 and YM158 plants at maturity. (g) ROS production in T-L8, T-L6, T-L1 and YM158 plant leaves infected with CWMV was analysed by DAB and NBT staining. YM158 was used as the control. (h) Measurement of the relative DAB and NBT staining intensity as shown in (g). Values were obtained by measuring three representative images chosen from three biological replicates, the data presented are the means \pm SD. Statistical analysis was performed using Student's *t*-test. **P* < 0.05. Bar, 10 cm. (i) CWMV incidence in YM158 and T-L8, T-L6, T-L1 plants in fields. (j) CWMV incidence in YM158 and T-L8, T-L6, T-L1 plants in laboratory. Mean \pm SD values are from three independent experiments with 45 plants per treatment, determined using the Student's *t*-test. **P* < 0.05.

Discussion

It is well known that THI1/THI2 plays a vital role in thiamine biosynthesis (Machado *et al.*, 1996). Recent studies have revealed that THI1 is a multifunctional protein. In *Arabidopsis*, THI1 is associated with protection against mitochondrial DNA damage and plays a key role in drought response by modulating ABA-induced

stomatal closure (Ajjawi *et al.*, 2007; Li *et al.*, 2016). Additionally, the expression of *THI1* is up-regulated under abiotic stresses (Abidin *et al.*, 2016; Rapalakozik *et al.*, 2012). However, the role of THI1 in plant responses to biotic stresses is still unknown. In this study, we cloned a THI1 orthologue named TaTHI2 from wheat, and sequencing of TaTHI2 revealed a close identity with homologous genes in other plant species (Figure 1a). Our results showed that

TaTHI2 is targeted to the chloroplast under the control of its native promoter (Figure 1c). Interestingly, the accumulation of TaTHI2 was found to be localized to the plasma membrane and increased in response to CWMV infection (Figure 2a–e). The significance of this change in the localization of TaTHI2 is unclear and warrants further research to study the function of membrane-localized TaTHI2 in response to biotic stress.

Here we present evidence that overexpression of *TaTHI2* in wheat reduced CWMV infection, while knocking down *TaTHI2* expression increased mosaic symptoms and CWMV accumulation (Figure 3a–f). These data suggest that TaTHI2 may play a crucial role in host resistance to CWMV infection. As TaTHI2 was found to be membrane-localized under CWMV infection and does not contain any membrane localization signal peptides, we speculate that its targeting to the plasma membrane is likely due to protein–protein interactions (Figure 2a–e). Indeed, TaTHI2 was found to interact with TaCPK5, a plasma membrane protein (Figure 4a–c), and to inhibit the autophosphorylation activity of TaCPK5 (Figure 4d,e). This phenomenon is similar to the repression of AtCPK33 autophosphorylation by the interaction between AtTHI1 and AtCPK33, as reported by Li *et al.* (2016). We propose that TaTHI2 enhances plant resistance to virus infection by interrupting the function of TaCPK5.

Plants can promote ROS accumulation by regulating ROS scavenging mechanisms in response to biotic stress. For example, a transcriptional repressor (Alfin-like 7, AL7) positively regulates plant resistance against tobacco mosaic virus (TMV) by restricting the expression of ROS scavenging genes in *N. benthamiana* (Zhang *et al.*, 2023a). Similarly, we found that TaTHI2 negatively regulates the phosphorylation of TaCAT1 by repressing the kinase activity of TaCPK5, which increases ROS concentration (Figures 5f and 6c–f). It is well known that ROS functions as signalling to activate the defense genes expression and defensive compound synthesis (Mittler *et al.*, 2022). Besides, ROS also act as a toxic agent to cause localized cell necrosis in the vicinity of the infection site, which restricts viral infection (Hakmaoui *et al.*, 2012). However, overexpression of *TaTHI2* in wheat only significantly reduced CWMV infection but not BSMV (Figures 3a–f and 56b), we suggested that TaTHI2 is specifically involved in wheat antiviral response to CWMV via ROS signalling.

During the coevolutionary arms race between viruses and plants, viruses have developed various strategies to disrupt plant defense pathways, such as interfering with the RNA silencing pathway and suppressing ROS production (Landeo-Ríos *et al.*, 2016; Mathioudakis *et al.*, 2013). These strategies to reduce ROS accumulation can be classified into preventing host ROS generation, promoting ROS clearance, and other pathways. For instance, the Barley stripe mosaic virus (BSMV) γ B protein interacts with glycolate oxidase (GOX) to inhibit ROS production and facilitate BSMV infection (Yang *et al.*, 2017). Similarly, the Chilli vein mottle virus (ChVMV) potyviral helper component proteinase (HCPPro) interacts with host catalase, increasing the level of ROS to promote viral infection (Yang *et al.*, 2020b). In this study, we found that CWMV CP can bind to TaTHI2 and resume the autophosphorylation of TaCPK5 by competitively interacting with TaTHI2 (Figure 7a–e). Moreover, we showed that overexpression of CWMV CP in wheat suppresses ROS production and enhances CWMV infection (Figure 8a–c,g–j). These findings suggest that CWMV CP interrupts the host defense response mediated by TaTHI2 to reduce ROS production, facilitating virus infection. Thus, our study adds further evidence to the coevolutionary arms race between viruses and plants.

Wheat is a major source of calories and protein, providing over 20% of the world's food supply. However, biotic and abiotic stresses pose significant threats to wheat production (Bailey-Serres *et al.*, 2019). In particular, Chinese wheat mosaic virus (CWMV) can cause severe yield losses, seriously impacting food security in China (Diao *et al.*, 1999). Thus, finding ways to protect wheat from CWMV infection is critical. Grain number and weight are important determinants of wheat yield (Li *et al.*, 2019), and in this study, we generated three overexpression TaTHI2 transgenic lines that showed resistance to CWMV infection (Figure 3d–f,j,k) as well as a 14%–18% increase in grain number and an 8%–11% increase in 1000-kernel weight in CWMV-contaminated soil (Figure 3i). Our results also showed that there is a potential positive relationship between the content of thiamine and wheat yield in these *TaTHI2*-OE wheat plants (Figures 4l,m and 57). These results suggest that overexpression of *TaTHI2* in wheat can not only confer resistance to CWMV but also improve yield, indicating a potential mechanism for yield improvement.

Thiamin plays vital roles as a coenzyme in redox reactions, which is involved in broad-spectrum resistance to many pathogens infection. Though thiamin content significantly increased in *TaTHI2*-OE wheat plants, the mosaic symptoms, as well as the accumulation level of BSMV CP in TaTHI2-OE plants was similar to that in YM158 after inoculating with BSMV (Figure 56b). These results suggested that the ROS homeostasis was indirectly regulated by thiamin in wheat. In addition, the previous study showed that the thiamine content may be related to the improved photosynthetic rate of plants resulting increase in grain yield (Bocobza *et al.*, 2013). In this study, overexpression of *TaTHI2* significantly improved wheat yield compared to YM158 in disease nursery (Figure 3g–i). Taken together, we putative thiamin plays vital roles as a coenzyme to improved the photosynthetic rate of plants but not as a factor to directly regulate the ROS homeostasis in wheat at least during CWMV infection.

In conclusion, our study proposes a model where TaTHI2 plays a crucial role in regulating ROS levels to inhibit CWMV infection (Figure 9a). During the early stages of infection, TaTHI2 represses

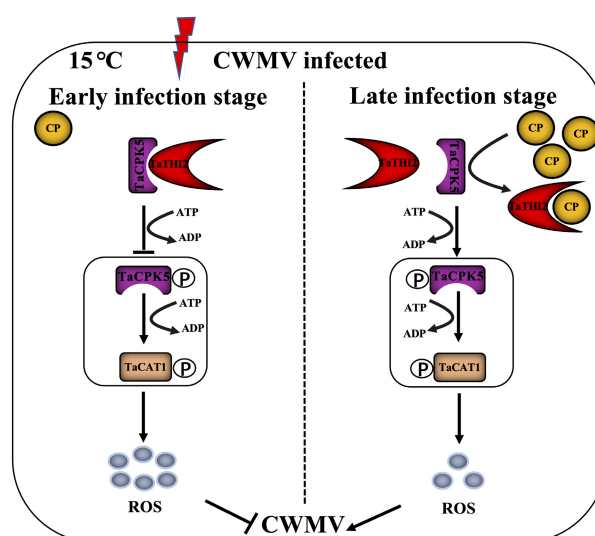


Figure 9 A proposed working model illustrating CWMV CP and TaTHI2-TaCPK5 module in plant-virus interaction. CWMV infection leads to the activation of the TaTHI2-mediated antiviral defense. CWMV CP disturbs this antiviral response.

TaCPK5-mediated TaCAT1 activity to increase ROS production and inhibit CWMV. However, as CWMV heavily accumulates in wheat, CWMV CP competitively binds to TaTHI2, leading to the resumption of TaCPK5 autophosphorylation and enhanced virus infection. Our findings reveal a new function of TaTHI2 in plant disease resistance and provide further evidence of the coevolutionary arms race between plants and viruses. Notably, TaTHI2 represents a valuable gene that can balance disease resistance and wheat yield.

Materials and methods

Plant materials and growth conditions

Nicotiana benthamiana plants were grown in soil inside a growth chamber maintained at $25 \pm 2^\circ\text{C}$, a 16 h light and 8 h dark photoperiod, and $65 \pm 5\%$ relative humidity. A CWMV-susceptible wheat cultivar, cv. Yangmai 158 (YM158), were used as controls. Wheat seedlings were grown inside a greenhouse set at $25 \pm 2^\circ\text{C}$. Four-leaf-stage wheat seedlings were rub-inoculated with CWMV and then grown in a growth chamber at 15°C with a 16 h light/8 h dark cycle. For field assessments, YM158 and the transgenic wheat lines were grown in a field nursery with a history of CWMV infection in Rongcheng, Shandong Province, China, from 2020 to 2023.

Plasmid construction

The full length of TaTHI2, TaCPK5 and TaCAT1 was cloned from Yangmai158 cDNA. The full length of PIP2A was cloned from Arabidopsis cDNA. TaTHI2 CDS cloned into the pGWB505, pGWB408, pCambia1300-nLUC, pCambia1300-cLUC, pET-32a, pGBKT7, pYES2 vectors, respectively. The upstream promoter region (~2 kb) of TaTHI2 was cloned into p35S:TaTHI2-GFP (pGWB505) and p35S:TaTHI2-His (pGWB408) plasmids in place of the 35S promoter to obtain pTHI2:TaTHI2-GFP and pTHI2:TaTHI2-His. The coding sequence of AtPIP2A was cloned into pGWB454. TaCPK5 was cloned into pGWB511, pGWB454, pGWB514, pGWB505, pCambia1300-cLUC, pCambia1300-nLUC, pGEX-4T-2 vectors, respectively. TaCAT1 CDS was cloned into pCambia1300-nLUC, pGWB514, pGWB505, pGWB511, pMAL-c2X vectors, respectively. TaCAT1(S258A) was cloned into pGWB505. CWMV CP was cloned into pGADT7, pCambia1300-cLUC, pMAL-c2X, pWMB190, pGWB454 vectors, respectively. All primers used in this study are listed in Table S3.

Virus inoculation and agroinfiltration

Inoculation of wheat seedlings with *in vitro* transcribed CWMV RNAs was performed as previously described (Yang *et al.*, 2020a). In brief, mechanically inoculated to the leaf 2 (bottom-up) of wheat seedlings with *in vitro* transcripts of CWMV and then the inoculated plants were grown inside a climate house at $15 \pm 2^\circ\text{C}$. Agroinfiltration using *Agrobacterium tumefaciens* (strain GV3101) was performed as described previously (Yang *et al.*, 2020a).

Subcellular fractionation assay

The leave samples were harvested and extracted for subcellular fractionation in the homogenization buffer (50 mM Tris-HCl, pH 8.0, 10 mM KCl, 3 mM MgCl₂, 1 mM EDTA, 1 mM DTT, 0.1% BSA, 0.3% dextran, and 13% (w/v) sucrose) as described in a previous study (Mei *et al.*, 2018). The sample was centrifugated at 3000 g for 20 min at 4°C . The resulting supernatant was collected and then centrifuged at 30 000 g for 1 h at 4°C to

generate the soluble (S) and the microsomal (P) fractions. The P fraction was resuspended again in the homogenization buffer. All fractions were analysed in SDS-PAGE/western blot analysis. The chloroplast proteins were extracted with the Minute™ Chloroplast Isolation Kit (Invent Biotechnologie) according to the methods provided by the manufacturer. The resulting samples were analysed in SDS-PAGE/western blot analysis.

Western blot assay

Total proteins were extracted from leaf tissues that were homogenized in a lysis buffer containing 6% SDS, 2% β -mercaptoethanol and 100 mM Tris-HCl (pH 8.8). Protein samples were mixed with SDS loading buffer individually and boiled for 8 min. Protein samples were separated in SDS-PAGE gels through electrophoresis and then transferred to nitrocellulose membranes. The blots were detected with specific primary antibodies, followed by an HRP-conjugated anti-mouse/anti-rabbit secondary antibody (Abbkine Scientific, California, USA).

BSMV-based VIGS

To silence *TaTHI2* expression in wheat, a 241 bp fragment from *TaTHI2* was cloned into the pBSMV γ vector. Plasmid DNAs (pBSMV α , pBSMV β , pBSMV γ , pBSMV γ :TaTHI2 and pBSMV γ :TaPDS) were linearized and transcribed *in vitro*, using specific restriction enzymes and the Message T7 *in vitro* transcription kit (Ambion, Austin, TX; Promega, Shenzhen, China) as instructed. The leave 2 (bottom-up) of wheat seedling at the two-leaf stage was rub-inoculated with BSMV(BSMV: γ , BSMV: TaPDS-as, BSMV: TaTHI2-as) as described previously (Yang *et al.*, 2020a). BSMV: TaPDS-inoculated plants were used as positive controls. The inoculated seedlings were grown inside a dark growth chamber at 25°C and humidity for 24 h, and then under a 16 h light/8 h dark photoperiod.

RNA extraction and qRT-PCR analysis

Total RNA was extracted from tissue samples using the HiPure plant RNA mini kit (Magen, Guangzhou, China). First-strand cDNA was synthesized with the First-Strand cDNA Synthesis Kit (TOYOBO, Osaka, Japan) according to the manufacturer's protocol. Quantitative PCR was performed using the SYBR Green qRT-PCR kit (Vazyme, Nanjing, China) on an ABI7900HT sequence detection system (Applied Biosystems, Foster City, CA, USA). At least three biological replicates were used for each treatment and each biological replicate has three technical replicates. The relative expression levels of assayed genes were calculated using the $2^{-\Delta\Delta C_t}$ method (Livak and Schmittgen, 2001). All primers for RT-PCR are listed in Table S3.

Wheat transformation

The constructed plasmids pCAMV35S:CP, pTHI2:TaTHI2-His and TaTHI2-pAHC25 were transformed into immature wheat embryos using particle bombardment, along with the vector pAHC20 containing a selective marker gene bar (bialaphos resistance gene), respectively. Generating transgenic wheat plants were selected as previously described (Chen *et al.*, 2014).

Wheat protoplast isolation and transfection

The CWMV infectious clones pCB-35S-R1 and pCB-35S-R2 were made previously (Yang *et al.*, 2016). Plasmids pCB-35S-R1 and pCB-35S-R2 contain full-length CWMV RNA1 and RNA2, respectively. The protoplasts were isolated from leaf blades and sheaths of 10- to 14-day-old wheat seedlings as previously

described (Yang *et al.*, 2020a). The plasmid pTHI2:TaTHI2-GFP was co-transfected into wheat protoplasts with pCB-35S-R1 and pCB-35S-R2 using a PEG-mediated transformation method (Bio-Rad, Hercules, CA, USA). The plasmid 35S:TaCPK5-GFP transfected into wheat protoplasts using the same method. The transfected protoplasts were washed twice with W5 solution and incubated at room temperature (RT) overnight in the dark. The protoplasts were harvested for protein extraction.

Co-immunoprecipitation assays

The agroinfiltrated *N. benthamiana* tissue samples were ground individually in protein IP buffer (50 mM Tris-HCl, pH 8.0, 150 mM NaCl, 2 mM EDTA, 1 mM dithiothreitol, 10% glycerol, 1% Triton X-100, 1 mM PMSF). The extract was centrifugated at 16 000 g for 20 min at 4 °C and the supernatant was collected. Then, supernatants incubated with twenty microliters of GFP-Trap_MA beads (Chromotek) for 2 h at 4 °C. The beads were washed at least four times with 1 × TBS buffer, and then SDS loading buffer were added for western blot analyses.

LCI assay

TaTHI2 CDS was cloned into pCambia1300-nluc and pCambia1300-cluc to produce TaTHI2-nluc and pLuc-TaTHI2. TaCPK5 CDS was cloned into pCambia1300-nluc and pCambia1300-cluc to produce TaCPK5-nluc and pLuc-TaCPK5. TaCAT1 CDS was cloned into pCambia1300-nluc to produce TaCAT1-nluc. CWMV CP was cloned into pCambia1300-cluc to produce pLuc-CP. These plasmids were separately transformed into *Agrobacterium* strain GV3101. After culturing and induction, *Agrobacterium* culture carrying pLuc-TaTHI2 was mixed in equal proportions with *Agrobacterium* culture carrying TaCPK5-nluc. *Agrobacterium* culture carrying pLuc-TaCPK5 was mixed in equal proportions with *Agrobacterium* culture carrying TaCAT1-nluc. *Agrobacterium* culture carrying pLuc-CP was mixed in equal proportions with *Agrobacterium* culture carrying TaTHI2-nluc. Then, the mixed *Agrobacterium* cultures infiltrated into *N. benthamiana* leaves individually. After 72 h, the leaves were incubated with a 0.2 mM luciferin (Thermo Scientific, USA) solution for 5 min and then observed under a chemiluminescence imaging system (Tanon). cLuc-TaTHI2+nLuc, cLuc-TaCPK5+nLuc, cLuc-CP+nLuc, cLuc+TaCPK5-nLuc, cLuc+TaCAT1-nLuc and cLuc+TaTHI2-nLuc were used as negative controls, cLuc-SAR+-sGF-nLuc were used as positive controls.

In vitro/vivo phosphorylation assay

In vitro phosphorylation assay, purified TaCPK5 (1 µg) and TaTHI2 (1 µg) were mixed in a 25 µL reaction buffer containing 25 mM Tris-HCl (pH 7.5), 10 mM MgCl₂, 1 mM DTT, 100 µM ATP at 25 °C for 30 min. In order to investigate whether TaTHI2 inhibit the autophosphorylation activity of TaCPK5, 1 µg of TaCPK5-GST was mixed with 0, 1, 10 and 30 µg of TaTHI2-His in reaction buffer at 25 °C for 30 min. To confirm TaCAT1 is a substrate of TaCPK5, purified TaCAT1-MBP (1 µg) was incubated with TaCPK5-GST (1 µg) in reaction buffer at 25 °C for 30 min. Reaction were stopped by adding 5× SDS loading buffer and boiled for 8 min. The reactions were analysed in SDS-PAGE gels, and phosphorylated proteins were detected using the pIMAGO kit (Tymora Analytical). Purified GST, His and MBP were used as a control.

In vivo phosphorylation assay, we co-expressed TaCPK5-HA and TaCAT1-GFP or TaCAT1^{S258A}-GFP in *N. benthamiana* leaves. The leaves expressing TaCAT1-GFP or TaCAT1^{S258A}-GFP were

used as a control. Total proteins were extracted at 72 h and enriched through immunoprecipitation (IP). The enriched CAT1-GFP/CAT1^{S258A}-GFP fusion was analysed through western blot using a phosphoserine-specific antibody (#ab9332; Abcam, Cambridge, MA, USA). Total protein extract was analysed through western blot using an anti-GFP/HA antibody (TransGen Biotech, Beijing, China).

Measurement of catalase activity assay

To investigate the role of TaCPK5 on TaCAT1 catalase activity in plants, we co-expressed TaCPK5-HA and TaCAT1-GFP or TaCAT1^{S258A}-GFP in *N. benthamiana* leaves. The leaves expressing TaCAT1-GFP or TaCAT1^{S258A}-GFP were used as a control. After 48 h, total proteins were extracted from these leaves and then analysis the catalase activity of CAT using a CAT assay kit (Beyotime) according to the manufacturer's instructions.

Detection of thiamine content

Measure thiamine content in the leaves of TaTHI2-OE wheat plants and 'YM158' wheat plants. The samples were ground in liquid nitrogen and 20 mL of the reagent mixture (0.1 mol/L hydrochloric acid:methanol, 20:80 v/v) was added to the sample and extracted in an ultrasonic cleaner for 30 min. The extracts were repeated under the same conditions three times. Then, these three extracts and concentrated by blowing with a nitrogen-blowing apparatus, and the volume was fixed to 0.5 mL and then followed by HPLC analysis. Thiamine levels measured by RUIYUAN Biotechnology Co., Ltd. Three biological replicates were used and each biological replicate has three technical replicates for thiamine quantification.

Histochemical staining of O₂^{•−} and H₂O₂

To detect O₂^{•−} and H₂O₂ accumulation, the infiltrated leaves were stained with NBT or DAB solution as described (Wu *et al.*, 2017). Briefly, the inoculated *N. benthamiana* or infected wheat leaves were harvested and stained in NBT (Solarbio) or DAB (Sigma) solution overnight in the dark. The relative NBT and DAB staining intensity was measured as described using IMAGEJ software (<http://rsbweb.nih.gov/ij>) (Sun and Folimonova, 2019).

Yeast two hybrid (YTH) assay

To confirm the interaction between CP and TaTHI2, pAD-CP and BD-TaTHI2 were co-transformed into yeast cells (strain Y2H Gold). The co-transformed cells were plated on SD (-Trp/-Leu) for 3 days and then plated on SD (-Ade/-His/-Leu/-Trp). Yeast cells co-transformed with AD-T+BD-Lam were used as a negative control. Yeast cells co-transformed with AD-T+BD-53 were used as a positive control.

CWMV CP/TaCPK5 competition assays for TaTHI2 binding

For the pull-down assay, the purified proteins (TaCPK5-GST, TaTHI2-His and CP-MBP) were co-incubated in a TBS (1×) buffer containing PMSF(1 mM) at 4 °C for 1 h. Addition of different gradient dilutions of CP-MBP (0, 1×, 2×, 4×, 6×) purified protein to the protein extracts of TaCPK5-GST and TaTHI2-His, and then were used in the His pull-down assay. After 1 h incubation, beads were washed four times with wash buffer (1× TBS, 0.05% Tween 20). Then, 5× SDS loading buffer was mixed with the washed beads and the washed beads were detected through western blot using anti-GST/His/MBP antibody (TransGen Biotech, Beijing, China).

In vitro phosphorylation assay, 1 µg of TaCPK5-GST and 10 µg of TaTHI2-His were mixed with 0, 1, 8 and 20 µg of CP-MBP in reaction buffer at 25 °C for 40 min. Reactions were stopped by adding 5 × SDS loading buffer and boiled for 8 min. The reactions were analysed in SDS–PAGE gels and phosphorylated proteins were detected using the pIMAGO kit (Tymora Analytical). Purified MBP was used as a control.

Acknowledgements

This work was supported by the Zhejiang Provincial Natural Science Foundation of China (grant no. LDQ23C140001), the China Agriculture Research System from the Ministry of Agriculture of the P.R. China (CARS-03), Foundation of Zhejiang Province High-level Talent Project (grant no. 2022R52022). We thank Zhensheng Kang (Northwest Agricultural and Forestry University, Yangling, Shaanxi Province, China) for providing the BSMV-based VIGS vector.

Conflict of Interest

The authors declare no conflict of interest.

Author Contributions

J. Y. (Jian Yang), J. C. designed experiments. J. Y., L. C., P. J., J. Z., P. L., X. C., J. L., T. Z., H. H., S. L., K. Z., and J. L. performed the experiments. All authors analysed and discussed the results. J. Y. (Jin Yang) and J. Y. (Jian Yang) wrote the manuscript.

References

- Abidin, A.Z., Wong, S.Y., Rahman, N.A., Idris, Z. and Yusof, Z.B. (2016) Osmotic, oxidative and salinity stresses upregulate the expressions of Thiamine (vitamin B1) biosynthesis genes (THIC and THI1/THI4) in oil palm (*Elaeis guineensis*). *J. Oil Palm Res.* **28**, 308–319.
- Ajjawi, I., Tsegaye, Y. and Shintani, D. (2007) Determination of the genetic, molecular, and biochemical basis of the *Arabidopsis thaliana* thiamin auxotroph th1. *Arch. Biochem. Biophys.* **459**, 107–114.
- Andika, I.B., Sun, L., Xiang, R., Li, J. and Chen, J. (2013a) Root-specific role for *Nicotiana benthamiana* RDR6 in the inhibition of Chinese wheat mosaic virus accumulation at higher temperatures. *Mol. Plant Microbe Interact.* **26**, 1165–1175.
- Andika, I.B., Zheng, S., Tan, Z., Sun, L., Kondo, H., Zhou, X. and Chen, J. (2013b) Endoplasmic reticulum export and vesicle formation of the movement protein of Chinese wheat mosaic virus are regulated by two transmembrane domains and depend on the secretory pathway. *Virology* **435**, 493–503.
- Bacete, L., Mérida, H., Miedes, E. and Molina, A. (2017) Plant cell wall-mediated immunity: cell wall changes trigger disease resistance responses. *Plant J.* **93**, 614–636.
- Bailey-Serres, J., Parker, J.E., Ainsworth, E.A., Oldroyd, G.E.D. and Schroeder, J.I. (2019) Genetic strategies for improving crop yields. *Nature* **575**, 109–118.
- Baulcombe, D. (2004) RNA silencing in plants. *Nature* **431**, 356–363.
- Bocobza, S.E., Malitsky, S., Araújo, W.L., Nunes-Nesi, A., Meir, S., Shapira, M., Fernie, A.R. et al. (2013) Orchestration of thiamin biosynthesis and central metabolism by combined action of the thiamin pyrophosphate riboswitch and the circadian clock in *Arabidopsis*. *Plant Cell* **25**, 288–307.
- Caplan, J., Padmanabhan, M. and Dinesh-Kumar, S. (2008) Plant NB-LRR immune receptors: from recognition to transcriptional reprogramming. *Cell Host Microbe* **3**, 126–135.
- Chabregas, S.M., Luche, D.D., Farias, L.P., Ribeiro, A.F., van Sluys, M.A., Menck, C.F. and Silva-Filho, M.C. (2001) Dual targeting properties of the N-terminal signal sequence of *Arabidopsis thaliana* THI1 protein to mitochondria and chloroplasts. *Plant Mol. Biol.* **46**, 639–650.
- Chang, M., Chen, H., Liu, F. and Fu, Z. (2021) PTI and ETI: convergent pathways with diverse elicitors. *Trends Plant Sci.* **27**, 113–115.
- Chen, M., Sun, L., Wu, H., Chen, J., Ma, Y., Zhang, X., Du, L. et al. (2014) Durable field resistance to wheat yellow mosaic virus in transgenic wheat containing the antisense virus polymerase gene. *Plant Biotechnol. J.* **12**, 447–456.
- Diao, A., Chen, J., Ye, R., Zheng, T., Yu, S., Antoniwi, J.F. and Adams, M.J. (1999) Complete sequence and genome properties of Chinese wheat mosaic virus, a new furovirus from China. *J. Gen. Virol.* **80**, 1141–1145.
- Fuji, S., Mochizuki, T., Okuda, M., Tsuda, S., Kagiwada, S., Sekine, K.T., Ugaki, M. et al. (2022) Plant viruses and viroids in Japan. *J. Gen. Plant Pathol.* **88**, 105–127.
- Goyer, A. (2010) Thiamine in plants: aspects of its metabolism and functions. *Phytochemistry* **71**, 1615–1624.
- Hakmaoui, A., Perez-Bueno, M.L., García-Fontana, B., Camejo, D., Jimenez, A., Sevilla, F. and Baron, M. (2012) Analysis of the antioxidant response of *Nicotiana benthamiana* to infection with two strains of pepper mild mottle virus. *J. Exp. Bot.* **63**, 5487–5496.
- Jones, J.D. and Dangl, J.L. (2006) The plant immune system. *Nature* **444**, 323–329.
- Landeo-Ríos, Y., Navas-Castillo, J., Moriones, E. and Cañizares, M. (2016) The p22 RNA silencing suppressor of the crinivirus Tomato chlorosis virus preferentially binds long dsRNAs preventing them from cleavage. *Virology* **488**, 129–136.
- Li, C.L., Wang, M., Wu, X.M., Chen, D.H., Lv, H.J., Shen, J.L., Qiao, Z. et al. (2016) THI1, a thiamine thiazole synthase, interacts with Ca²⁺-dependent protein kinase CPK33 and modulates the S-type anion channels and stomatal closure in *Arabidopsis*. *Plant Physiol.* **170**, 1090–1104.
- Li, N., Xu, R. and Li, Y. (2019) Molecular networks of seed size control in plants. *Annu. Rev. Plant Biol.* **70**, 435–463.
- Li, P., Zhao, L., Qi, F., Htwe, N., Li, Q., Zhang, D., Lin, F. et al. (2021) The receptor-like cytoplasmic kinase RIPK regulates broad-spectrum ROS signaling in multiple layers of plant immune system. *Mol. Plant* **14**, 1652–1667.
- Li, J., Feng, H., Liu, S., Liu, P., Chen, X., Yang, J., He, L. et al. (2022) Phosphorylated viral protein evades plant immunity through interfering the function of RNA-binding protein. *PLoS Pathog.* **18**, e1010412.
- Livak, K.J. and Schmittgen, T.D. (2001) Analysis of relative gene expression data using real-time quantitative PCR and the 2^{−ΔΔCT} method. *Methods* **25**, 402–408.
- Machado, C.R., Oliveira, R.L.C.D., Boiteux, S., Praekelt, U.M. and Menck, C.F.M. (1996) Thi1, a thiamine biosynthetic gene in *Arabidopsis thaliana*, complements bacterial defects in DNA repair. *Plant Mol. Biol.* **31**, 585–593.
- Maejima, H., Taniguchi, T., Watarai, A. and Katsuoka, K. (2010) Evaluation of nail disease in psoriasis arthritis by using a modified nail psoriasis severity score index. *Int. J. Dermatol.* **49**, 901–906.
- Marmagne, A., Rouet, M.A., Ferro, M., Rolland, N., Alcon, C., Joyard, J., Garin, J. et al. (2004) Identification of new intrinsic proteins in *Arabidopsis* plasma membrane proteome. *Mol. Cell. Proteomics* **3**, 675–691.
- Mathioudakis, M.M., Veiga, R.S., Canto, T., Medina, V., Mossialos, D., Makris, A.M. and Livieratos, I. (2013) Pepino mosaic virus triple gene block protein 1 (TGBp1) interacts with and increases tomato catalase 1 activity to enhance virus accumulation. *Mol. Plant Pathol.* **14**, 589–601.
- Mei, Y., Yang, X., Huang, C., Zhang, X. and Zhou, X. (2018) Tomato leaf curl Yunnan virus-encoded C4 induces cell division through enhancing stability of Cyclin D 1.1 via impairing NbSK1-mediated phosphorylation in *Nicotiana benthamiana*. *PLoS Pathog.* **14**, e1006789.
- Mittler, R. (2016) ROS are good. *Trends Plant Sci.* **22**, 11–19.
- Mittler, R., Zandalinas, S.I., Fichman, Y. and Van Breusegem, F. (2022) Reactive oxygen species signalling in plant stress responses. *Nat. Rev. Mol. Cell Biol.* **23**, 663–679.
- Rapalakozik, M., Wolak, N., Kujda, M. and Banas, A.K. (2012) The upregulation of thiamine (vitamin B1) biosynthesis in *Arabidopsis thaliana* seedlings under salt and osmotic stress conditions is mediated by abscisic acid at the early stages of this stress response. *BMC Plant Biol.* **12**, 2.
- Strobbe, S., Verstraete, J., Fitzpatrick, T.B., Faustino, M., Lourenço, T.F., Oliveira, M.M., Stove, C. et al. (2022) A novel panel of yeast assays for the assessment of thiamin and its biosynthetic intermediates in plant tissues. *New Phytol.* **234**, 748–763.

- Sun, Y.D. and Folimonova, S.Y. (2019) The p33 protein of Citrus tristeza virus affects viral pathogenicity by modulating a host immune response. *New Phytol.* **221**, 2039–2053.
- Sun, L., Andika, I.B., Shen, J., Yang, D., Ratti, C. and Chen, J. (2013) The CUG-initiated larger form coat protein of Chinese wheat mosaic virus binds to the cysteine-rich RNA silencing suppressor. *Virus Res.* **177**, 66–74.
- Tunc-Ozdemir, M., Miller, G., Song, L., Kim, J., Sodek, A., Koussevitzky, S., Misra, A.N. *et al.* (2009) Thiamin confers enhanced tolerance to oxidative stress in Arabidopsis. *Plant Physiol.* **151**, 421–432.
- Wu, J., Yang, R., Yang, Z., Yao, S., Zhao, S., Wang, Y., Li, P. *et al.* (2017) ROS accumulation and antiviral defence control by microRNA528 in rice. *Nat. Plants* **3**, 16203.
- Yang, J., Zhang, F., Xie, L., Song, X.J., Li, J., Chen, J.P. and Zhang, H.M. (2016) Functional identification of two minor capsid proteins from Chinese wheat mosaic virus using its infectious full-length cDNA clones. *J. Gen. Virol.* **97**, 2441–2450.
- Yang, M., Li, Z., Zhang, K., Zhang, X., Zhang, Y., Wang, X., Han, C. *et al.* (2017) Barley stripe mosaic virus γ b interacts with glycolate oxidase and inhibits peroxisomal ROS production to facilitate virus infection. *Mol. Plant* **11**, 338–341.
- Yang, J., Zhang, T., Li, J., Wu, N., Wu, G., Yang, J., Chen, X. *et al.* (2020a) Chinese wheat mosaic virus-derived vsiRNA-20 can regulate virus infection in wheat through inhibition of vacuolar- (H(+))-PPase induced cell death. *New Phytol.* **226**, 205–220.
- Yang, T., Qiu, L., Huang, W., Xu, Q., Zou, J., Peng, Q., Lin, H. *et al.* (2020b) Chilli veinal mottle virus HCPro interacts with catalase to facilitate virus infection in *Nicotiana tabacum*. *J. Exp. Bot.* **71**, 5656–5668.
- Yang, J., Liu, P., Zhong, K., Ge, T., Chen, L., Hu, H., Zhang, T. *et al.* (2022) Advances in understanding the soil-borne viruses of wheat: from the laboratory bench to strategies for disease control in the field. *Phytopathol. Res.* **4**, 27.
- Zhang, D., Gao, Z., Zhang, H., Yang, Y., Yang, X., Zhao, X., Guo, H. *et al.* (2023a) The MAPK-Alfin-like 7 module negatively regulates ROS scavenging genes to promote NLR-mediated immunity. *Proc. Natl. Acad. Sci. USA* **120**, e2214750120.
- Zhang, T., Hu, H., Wang, Z., Feng, T., Yu, L., Zhang, J., Gao, W. *et al.* (2023b) Wheat yellow mosaic virus Nlb targets TaVTC2 to elicit broad-spectrum pathogen resistance in wheat. *Plant Biotechnol. J.* **21**, 1073–1088.

Supporting information

Additional supporting information may be found online in the Supporting Information section at the end of the article.

Table S1 LC–MS/MS analysis of TaTHI2 candidate interacting protein.

Table S2 The complete phospho-peptide sequences and mass-to-charge ratio (m/z) from the mass spectrum assay.

Table S3 Primers used in this research.

Figure S1 Alignment using three TaTHI2 sequences.

Figure S2 Colocalization of pTHI2:TaTHI2-GFP with PIP2A-RFP at 15 °C in *N. benthamiana* leaves infected with CWMV.

Figure S3 Analyses of *TaTHI2* mRNA expressions in *TaTHI2*-RNAi plants.

Figure S4 Functional analysis of TaTHI2 in wheat resistance to CWMV.

Figure S5 Analyses of TaTHI2 protein expressions in wheat plants.

Figure S6 Analyses of broad-spectrum virus resistance in *TaTHI2*-OE plants.

Figure S7 Field assessment of transgenic lines of *TaTHI2*-OE for agronomic traits in 2013.

Figure S8 Colocalization of pTHI2:TaTHI2-GFP with TaCPK5-RFP at 15 °C in *N. benthamiana* leaves.

Figure S9 Analyses of *TaCPK5* mRNA expressions in *TaTHI2*-OE transgenic wheat lines.

Figure S10 TaCPK5 positively regulates TaCAT1 catalase activity.

Figure S11 Different concentrations of GFP do not affect the accumulation of H₂O₂.

Figure S12 Colocalization of pTHI2:TaTHI2-GFP with CP-RFP at 15 °C in *N. benthamiana* leaves.

Figure S13 Eight wheat plants of T-L8, T-L6 and T-L1 were detected by RT-PCR in T3 generation.